Volcanic Eruptions: Cyclicity During Lava Dome Growth

Oleg Melnik[a,b] , R. Stephen J. Sparks[b], Antonio Costa[b,c], Alexei A. Barmin[a]

[a]Institute of Mechanics, Moscow State University, Russia

[b]Earth Science Department, University of Bristol, UK

[c]Istituto Nazionale di Geofisica e Vulcanologia, Naples, Italy.

ARTICLE OUTLINE

Glossary

andesite magma or volcanic rock is characterised by intermediate SiO_2 concentration. Andesite magmas have rheological properties that are intermediate between basalt and rhyolite magmas. Silica content in andesites ranges from approximately 52 to 66 weight percent. Common minerals in andesite include plagioclase, amphibole and pyroxene. Andesite is typically erupted at temperatures between 800 to 1000 ◦C Andesite is particularly common in subduction zones, where tectonic plates converge and water is introduced into the mantle.

basalt magma or volcanic rock contains not more than about 52% SiO_2 by weight. Basaltic magmas have a low viscosity. Volcanic gases can escape easily without generating high eruption columns. Basalt is typically erupted at temperatures between 1100 to 1250 ◦C. Basalt flows cover about 70% of the Earth's surface and huge areas of the terrestrial planets and so are the most important of all crustal igneous rocks.

Bingham liquid is a fluid that does not flow in response to an applied stress until a critical yield stress is reached. Above the critical yield stress, strain rate is proportional to the applied stress, as in a Newtonian fluid.

bubbly flow A multi-phase flow regime, in which the gas phase appears as bubbles suspended in a continuous liquid phase.

conduit A channel, through which magma flows towards the Earth's surface. Volcanic conduits can commonly be approximately cylindrical and typically a few 10's metres across or bounded by near parallel sides in a magma-filled fracture. Conduits can be vertical or inclined.

crystallisation conversion, partial or total, of a silicate melt into crystals during solidification of magma.

degassing n. (degas v.) The process by which volatiles that are dissolved in silicate melts come out of solution in the form of bubbles. Open- and closed-system degassing can be distinguished. In the former, volatiles can be lost or gained by the system. In the latter, the total amount of volatiles in the bubbles and in solution in the magma is conserved.

differentiation The process of changing the chemical composition of magma by processes of crystallization accompanied by separation melts from crystals.

dome A steep-sided, commonly bulbous extrusion of lava or shallow intrusion (cryptodome). Domes are commonly, but not exclusively, composed of SiO_2–rich magmas. In dome-forming eruptions the erupted magma is so viscous, or the discharge rate so slow, that lava accumulates very close to the vent region, rather than flowing away. Pyroclastic flows can be generated by collapse of lava domes. Recent eruptions producing lava domes include the 1995-2006 eruption of the Soufrière Hills volcano, Montserrat, and the 2004-2006 eruption of Mount St. Helens, USA.

dyke A sheet-like igneous intrusion, commonly vertical or near vertical, that cuts across pre-existing, older, geological structures. During magmatism, dykes transport magma toward the surface or laterally in fracture-like conduits. In the geologic record, dykes are preserved as sheet-like bodies of igneous rocks.

explosive eruption A volcanic eruption in which gas expansion tears the magma into numerous fragments with a wide range of sizes. The mixture of gas and entrained fragments flows upward and outward from volcanic vents at high speed into the atmosphere. Depending on the volume of erupted material, eruption intensity and sustainability, explosive eruptions are classified as Strombolian, Vulcanian, sub-Plinian, Plinian or Mega-Plinian; this order is approximately in the order of increasing intensity. Strombolian and Vulcanian eruptions involve very short-lived explosions.

extrusive flow or eruption A non-explosive (non-pyroclastic) magma flow from a volcanic conduit during a lava dome-building eruption or lava flow.

mafic Magma, lava, or tephra with silica concentrations of approximately SiO2 < 55%.

magma Molten rock that consists of up three components: liquid silicate melt, suspended crystalline solids, and gas bubbles. It is the raw material of all volcanic processes. Silicate magmas are the most common magma type and consist of long, polymeric chains and rings of Si − O tetrahedra, between which are located cations (e.g. Ca2+, Mg2+, Fe2+, and Na+). Anions (e.g. OH−, F−, Cl−, and S−) can substitute for the oxygen in the silicate framework. The greater the silica (SiO_2) content of the magma, the more chains and rings of silicate tetrahedra there are to impede each other and hence the viscosity of the magma increases. The pressure regime and composition of the magma control the minerals that nucleate and crystallize from a magma when it cools or degasses.

magma chamber A subsurface volume within which magma accumulates, differentiates and crystallizes. Igneous intrusions can constrain the form and size of some magma chambers, but in general the shape and volume of magma chambers beneath active volcanoes are poorly known. Magma reservoir is an equivalent term.

melt Liquid part of magma. Melts (usually silicate) contain variable amounts of dissolved volatiles. The primary volatiles are usually water and carbon dioxide.

Newtonian liquid A liquid for which the strain rate is proportional to the applied stress. The proportionality coefficient is called the viscosity.

microlite Crystal with dimensions less than 100 μm. Usually microlites crystallize at shallow levels of magmatic system.

phenocryst Crystal with dimensions larger than 100 μm. Usually phenocrysts grow in magmatic reservoirs prior to an eruption and or are entrained by magma in the chamber.

pyroclastic flow or surge A gas-particle flow of pyroclasts suspended in a mixture of hot air, magmatic gas, and fine ash. The flow originates by the gravitational collapse of a dense, turbulent explosive eruption column at the source vent, or by dome collapse, and moves down-slope as a coherent flow. Pyroclastic flows and surges are distinguished by particle concentration in the flow, surges being more dilute. Variations in particle concentration result in differences in the deposits left by flows and surges.

silicic Magma, lava, or tephra with silica concentrations of approximately $SiO_2 > 55\%$. The magmas are commonly rich in Al, Na− and K− bearing minerals. Silicic magmas are typically very viscous and can have high volatile contents. Rhyolite is an example of a silicic magma.

volatile A component in a magmatic melt which can be partitioned in the gas phase in significant amounts during some stage of magma history. The most common volatile in magmas is water vapour H_2O, but there are commonly also significant quantities of CO_2, SO_2 and halogens.

I. Definition of the Subject

We consider the process of slow extrusion of very viscous magma that forms lava domes. Dome-building eruptions are commonly associated with hazardous phenomena, including pyroclastic flows generated by dome collapses, explosive eruptions and volcanic blasts. These eruptions commonly display fairly regular alternations between periods of high and low or no activity with time scales from hours to years. Usually hazardous phenomena are associated with periods of high magma discharge rate, thus, understanding the causes of pulsatory activity during extrusive eruptions is an important step towards forecasting volcanic behaviour, especially the transition to explosive activity when magma discharge rate increases by a few orders of magnitude. In recent years the risks have increased because the population density in the vicinity of many active volcanoes has increased.

II. Introduction

Many volcanic eruptions involve the formation of lava domes, which are extrusions of very viscous, degassed magmas. The magma is so viscous that it accumulates close to the vent. Extrusion of lava domes is a slow and long-lived process, and can continue for many years or even decades [71, 83, 85]. Typical horizontal dimensions of lava domes are several hundred metres, heights are of an order of tens to several hundred meters, and volumes several million to hundreds of million cubic meters. Typical magma discharge rates (measured as the increase of dome volume with time in dense rock equivalent (DRE)) can reach up to 20-40 m^3/s, but are usually below 10 m^3/s [83].

Dome-building eruptions are commonly associated with hazardous phenomena, including pyroclastic flows and tsunamis generated by dome collapses, explosive eruptions and volcanic blasts. Dome-building eruptions can also contribute to edifice instability and sector collapse, as occurred on Montserrat on 26 December 1997 [87]. Lava dome activity can sometimes precede or follow major explosive eruptions; the eruption of Pinatubo, Philippines (1991) is an example of the former [37], and the eruption of Mount St. Helens, USA (1980-1986) is an example of the latter [89].

Several lava dome eruptions have been documented in detail and show quite complex behaviours. Substantial fluctuations in magma discharge rate have been documented. In some cases these fluctuations can be quite regular (nearly periodic), as in the extrusion of lava in 1980-1982 on Mount St. Helens [89] and in the 1922-2002 activity of the Santiaguito lava dome, Guatemala [35]. In these cases, periods of high magma discharge rate alternate with longer periods of low magma discharge rate or no extrusion. In some volcanoes, such as Shiveluch, Kamchatka, the intervals of no extrusion are so long compared with the periods of dome growth that the episodes of dome growth have been described as separate eruptions of the volcano rather than episodes of the same eruption. Other dome-building activity can be nearly continuous and relatively steady, as observed at Mount St. Helens in 1983 [89] and at the Soufrière Hills Volcano, Montserrat between November 1999 and July 2003. In yet other cases the behaviour can be more complex with quite sudden changes in magma

discharge rate, which cannot be related to any well-defined regularity or pattern (e.g. Lascar volcano, Chile, [57]).

Pauses during lava dome-building eruptions are quite common. For example, at Mount St Helens there were 9 pulses of dome growth with a period of ~74 days, a duration of 1-7 days and no growth in between [89]. The Soufrière Hills Volcano Montserrat experienced a long (20 months) pause in extrusion after the first episode of growth [72]. On Shiveluch volcano in Kamchatka episodes of dome growth occurred in 1980, 1993 and 2000, following a major explosion in 1964 [28]. Each episode of dome growth began with magma discharge rate increasing over the first few weeks to a peak of 8-15 m^3/s, with a gradual decline in magma discharge rate over the following year. In between the episodes very minimal activity was recorded.

Fluctuations in magma discharge rate have been documented on a variety of time-scales from both qualitative and quantitative observations. Several lava dome eruptions are characterized by extrusion of multiple lobes and flow units [68, 94]. In the case of the Soufrière Hills Volcano, extrusion of shear lobes can be related to spurts in discharge rate and is associated with other geophysical changes, such as onset of seismic swarms and marked changes in temporal patterns of ground tilt [90, 91, 94]. These spurts in discharge rate have been fairly regular for substantial periods, occurring every 6 to 7 weeks over a 7 month period in 1997 [91, 87, 21]. These spurts are commonly associated with large dome collapses and pyroclastic flows and, in some cases, with the onset of periods of repetitive Vulcanian explosions [14, 26]. Consequently the recognition of this pattern has become significant for forecasting activity for hazard assessment purposes. In the Soufrière Hills Volcano and Mount Pinatubo much shorter fluctuations in magma discharge rate have been recognized from cyclic variations in seismicity, ground tilt, gas fluxes and rock-fall activity [23, 91, 93]. This cyclic activity has typical periods in the range of 4 to 36 hours. Cyclic activity has been attributed to cycles of gas pressurization and depressurization with surges in dome growth related to degassing, rheological stiffening and stick-slip behaviour [23, 61, 91, 98, 49].

Dome eruptions can show transitions to explosive activity, which sometimes can be linked to spurts in magma discharge rate. For example, in 1980, periodic episodes of lava dome extrusion on Mount St. Helens were initiated by explosive eruptions, which partly destroyed the dome that had been extruded in each previous extrusion episode [89]. At Unzen Volcano, Japan a single Vulcanian explosive eruption occurred in June 1991 when the magma discharge rate was at its highest [68]. At the Soufrière Hills Volcano, repetitive series of Vulcanian explosions have occurred following large dome collapses in periods when magma discharge rates were the highest of the eruption [88, 26]. In the case of Lascar Volcano, Chile, an intense Plinian explosive eruption occurred on 18 and 19 April, 1993, after nine years of dome extrusion and occasional short-lived Vulcanian explosions [57].

Lava dome eruptions require magma with special physical properties. In order to produce a lava dome rather than a lava flow, the viscosity of the magma must be extremely high so that the lava cannot flow easily from the vent. High viscosity is a consequence of factors such as relatively low temperature (typically 750-900^{0}C), melt compositions rich in network-forming components (principally Si and Al) efficient gas loss during magma decompression, and crystallization as a response to cooling and degassing. Viscosities of silica-rich magmas, such as rhyolites and some andesites, are increased by several orders of magnitude by the loss of dissolved water during decompression. Many, but not all, domes also have high crystal content (up to 60 to 95 vol%), with crystallization being triggered mostly by degassing [10, 86]. In order to avoid fragmentation that leads to an explosive eruption, magma must have lost gas during ascent. Consider, for example, a magma at 150 MPa containing 5wt% of dissolved water decompressed to atmospheric pressure. Without gas loss the volume fraction of bubbles, will be more than 99 %. Typical dome rock contains less than 20 vol% of bubbles, although there is evidence that magma at depth can be more bubble-rich (e.g., [74, 13]). On the other hand, very commonly there is no change in temperature or bulk magma composition in the products of explosive and extrusive eruptions for a particular volcano. This suggests that the properties of magma that are conducive to the formation of lava domes are controlled by physico-chemical transformations that occurred during magma ascent to the surface.

Two other important factors that influence whether lava domes or flows form are topography and discharge rate. The same magma can form a dome if the discharge rate is low, and a lava flow if the rate is high [92, 29]. The discharge rate is controlled by overall conduit resistance that is a function

of viscosity, conduit size and shape, and driving pressure (the difference between chamber pressure and atmospheric pressure). Additionally the same magma can form a dome on low slopes, such as a flat crater (e.g. the mafic andesite dome of the Soufrière Volcano, St Vincent; [40]) and a lava flow on steep slopes.

Prior to an eruption, magma is usually stored in a shallow crustal reservoir called a magma chamber. For several volcanoes magma chambers can be detected and characterised by earthquake locations, seismic tomography, petrology or interpretation of ground deformation data [55]. Typical depths of magma chambers range from a few kilometres to tens of kilometres. Volumes range from less than one to several thousand km^3 [55], but are usually less than a hundred km^3. Magma chambers are connected to the surface by magma pathways called conduits. There is evidence that the conduits that feed lava dome eruptions can be both dykes or cylindrical. Dykes of a few meters width are commonly observed in the interior of eroded andesite volcanoes. Dyke feeders to lava domes have been intersected by drilling at Inyo crater, California, USA [56] and at Mount Unzen [67]. Geophysical studies point to dyke feeders; for example fault-plane solutions of shallow volcano-tectonic earthquakes indicate pressure fluctuations in dykes [75, 76]. Deformation data at Unzen, combined with structural analysis, indicate that the 1991-1995 dome was fed by a dyke [68]. Dykes are also the only viable mechanism of developing a pathway through brittle crust from a deep magma chamber to the surface in the initial stages of an eruption [77, 50].

Cylindrical conduits commonly develop during lava dome eruptions. The early stages of lava dome eruptions frequently involve phreatic and phreatomagmatic explosions that create near surface craters and cylindrical conduits [73, 99, 12, 89, 96, 87]. These explosions are usually attributed to interaction of magma rising along a dyke with ground water. Cylindrical conduits formed by explosions are confined to relatively shallow parts of the crust, probably of order hundreds of metres depth and < 1 km, as indicated by mineralogical studies [73]. Examples of such initial conduit forming activity include Mount Usu (Japan) Mt. St. Helens, and Soufrière Hills Volcano [99, 12, 87]. Many lava dome eruptions are also characterized by Vulcanian, sub-Plinian and even Plinian explosive eruptions. Examples include Mount Unzen, Mount St Helens, Santiaguito and Soufrière Hills Volcano [68, 89, 96, 87]. Here the fragmentation front may reach to depths of several kilometres [54] with the possibility of cylindrical conduit development due to severe underpressurization and mechanical disruption of conduit wallrocks. Subsequently domes can be preferentially fed along the cylindrical conduits created by earlier explosive activity. On the Soufrière Hills Volcano, early dome growth was characterised by extrusion of spines with nearly cylindrical shape [87].

Observations of magma discharge rate variations on a variety of time-scales highlight the need to understand the underlying dynamic controls. Research has increasingly focused on modelling studies of conduit flow dynamics during lava-dome eruptions. We will restrict our discussions here to mechanisms that lead to cyclic and quasi-periodic fluctuations in magma discharge rate on various timescales, mainly focusing on long-term cycles. Issues concerning the transition between explosive and extrusive activity are discussed in detail in [80, 81, 45, 97] and in the special volume of Journal of Volcanology and Geothermal Research dedicated to modelling of explosive eruptions [79]. Several papers consider the processes that occur at the surface and relate dome morphology and dimensions with controlling parameters.

Combined theoretical, experimental and geological studies identify four main types of dome: spiny, lobate, platy, and axisymmetric [5, 29, 30]. These types of dome reflect different regimes which are controlled by discharge rates, cooling rates and yield strength, and the viscosity of the dome-forming material. In recent years mathematical modelling has been used to semi-quantitatively describe spreading of lava domes, including models based on the thin layer approximation [1, 2] and fully 2D simulations of lava dome growth which account for visco-elastic and -plastic rheologies [32, 33].

III. Dynamics of magma ascent during extrusive eruptions.

In order to understand the causes of cyclic behaviour during extrusive eruptions, first we need to consider the underling dynamics of volcanic systems, and discuss physical and chemical transitions during magma ascent.

place figure 1 here

The physical framework for the model of a volcanic system is shown in Figure 1. Magma is stored in a chamber at depth L, with a chamber pressure P_{ch} that is higher than hydrostatic pressure of magma column and drives magma ascent. Magma contains silicate melt, crystals and dissolved and possibly exsolved volatiles. During ascent of the magma up the conduit the pressure decreases and volatiles exsolve forming bubbles. As the bubble concentration becomes substantial, bubble coalescence take place and permeability develops [27, 45], allowing gas to escape from ascending magma, both in vertical (through the magma) and horizontal (to conduit wallrocks) directions. If magma ascends slowly, gas escape results in a significant reduction of the volume fraction of bubbles; such a process is termed open system degassing. In comparison closed system degassing is characterized by a negligible gas escape. Reduction in bubble content, combined with relatively low gas pressures and efficient decoupling of the gas and melt phases, prevents magma fragmentation and, thus, development of explosive eruption [59, 60, 82].

Due to typical low ascent velocities (from millimetres to a few centimetres per second) magma ascent times to the Earth's surface from the magma chamber range from a several hours to many weeks. These ascent times are often comparable with the times that are required for crystals to grow significantly and for heat exchange between magma and wallrocks. The main driving force for crystallization is related to exsolution of volatiles from the magma, leading to increase in the liquidus temperature T_L, and development of magma undercooling $\Delta T = T_L - T$ [10]. Crystallization leads to release of latent heat, and magma temperature can increase with respect to the initial temperature [6]. As a consequence of increasing crystal content, magma viscosity increases by several orders of magnitude [16, 20, 21] and magma becomes a non-Newtonian fluid [78]. As will be shown later, crystallization induced by degassing can become a key process in causing variable flow rates.

Due to the long duration of extrusive eruptions, the magma chamber can be replenished with significant amounts of magma from underlying sources [65, 41]. Replenishment can lead to pressure build-up in the magma chamber, volatile and heat exchange between host and new magmas. The composition of the magma can also change over time, due to differentiation, crustal rock assimilation, or magma mixing. Thus, any model that explains magma ascent dynamics needs to deal with many complexities. Of course there is no single model that can take into account all physical processes in a volcanic system. Additional complications arise from the fact that the physical properties of magma at high crystal contents, such as rheology or crystal growth kinetics and geometry of volcanic systems, are typically poorly constrained. Several issues regarding the dynamics of multiphase systems have not been resolved theoretically, especially for cases where the volume fractions of components of the multiphase system are comparable.

Below we will present a review of existing models that treat cyclic behaviour during extrusive eruptions on different timescales.

IV. Short-term cycles.

Cyclic patterns of seismicity, ground deformation and volcanic activity (Figure 2 from [23]) have been documented at Mount Pinatubo, Philippines, in 1991 [37] and Soufrière Hills volcano, Montserrat, British West Indies, in 1996–1997 [90, 91]. At Soufrière Hills, periodicity in seismicity and tilt ranged from ~4 to 30 h, and the oscillations in both records continued for weeks. Cyclic behaviour was first observed in the seismicity (RSAM) records beginning in July 1996, when the record of dome growth constrained the average supply rate to between 2 and 3 m^3/s [88]. The oscillations in the RSAM records initially had low amplitudes, and no tilt-measurement station was close enough to the vent to detect any pressure oscillations in the conduit. By August 1996, RSAM records showed strong oscillatory seismicity at dome-growth rates between 3 and 4 m^3/s. Tilt data, taken close enough to the vent (i.e., Chances Peak [90]) to be sensitive to conduit pressure oscillations, are only available for February1997 and May–August 1997. In the latter period dome growth rate increase from ~5 m^3/s in May to between 6 and 10 m^3/s in August. Both near-vent tilt and RSAM displayed oscillatory behaviour during this period and were strongly correlated in time. Similar RSAM oscillations having periods of 7 to 10 h were observed at Mount Pinatubo following

the climactic eruption in 1991 [37]. At both volcanoes, oscillation periods were observed that do not fit any multiple of Earth or ocean tides.

place figure 2 here

The cyclic activity at both Pinatubo and Soufrière Hills Volcano are strongly correlated with eruptive behaviour and other geophysical phenomena. In the Pinatubo case and on Soufrière Hills Volcano in August, September and October 1997, the cycles were linked to short-lived volcanic explosions. In the case of the Soufrière Hills Volcano, explosions in August 1997 occurred at the peak in the tilt. The peak in tilt also marked the onset of episodes of increased rock falls [7, 8] and [91] is attributed to increased magma discharge rates. SO_2 flux data show that the cycles are linked to surges in gas release, which reach a peak about an hour after the tilt peak [93]. Green *et al*. [31] have shown that several families of near identical long period earthquakes occur during the tilt cycle, starting at the inflexion point on the up-cycle and finishing before the inflexion point on the down-cycle.

Several models [23, 98, 23, 98, 70, 49] have been proposed to explain the observed cyclicity. In these models [23, 98] the conduit is divided into two parts. Magma is assumed to be forced into the lower part of volcanic conduit at a constant rate. In Denlinger and Hoblitt [23] magma in the lower part of the conduit is assumed to be compressible. In Wylie *et al.* [98] the magma is incompressible but the cylindrical conduit is allowed to expand elastically. In both models the lower part of the conduit, therefore, acts like a capacitor that allows magma to be stored temporally in order to release it during the intense phase of the eruption. In the upper part of the conduit friction is dependent on magma discharge rate, with a decrease in friction resulting in an increase in discharge rate, over a certain range of discharge rates. In Denlinger and Hoblitt [23], when magma discharge rate reaches a critical value, magma detaches from the conduit walls and a stick-slip transition occurs. Rapid motion of magma leads to depressurization of the conduit and a consequent decrease in discharge rate, until at another critical value the magma again sticks to the walls. Pressure starts to increase again due to influx of new magma into the conduit. On a pressure-discharge diagram the path of eruption is represented by a hysteresis loop. In Wylie *et al.* [98] the friction is controlled by volatile-dependent viscosity. Volatile exsolution delay is controlled by diffusion. When magma ascends rapidly, volatiles have no time to exsolve and viscosity remains low. Depressurization of the upper part of the conduit leads to a decrease in magma discharge rate and an increase in viscosity due to more intense volatile exsolution.

In Neuberg *et al.* [70] a steady 2D conduit flow model was developed. The full set of Navier-Stokes equations for a compressible fluid with variable viscosity was solved by means of a finite element code. Below some critical depth the flow was considered to be viscous and Newtonian, with a no-slip boundary condition at the wall. Above this depth a plug develops, with a wall boundary condition of frictional slip. The slip criterion was based on the assumption that the shear stress inside the magma overcomes some critical value. Simulations reveal that slip occurs in the shallow part of the conduit, in good agreement with locations of long-period volcanic earthquakes for the Soufrière Hills Volcano, [31]. However, some parameters used in the simulations (low crystallinity, less than 30 % and high discharge rate, more than 100 m^3/s) are inconsistent with observations.

Lensky *et al.* [49] developed the stick-slip model by incorporating degassing from supersaturated magma together with a sticking plug. Gas diffuses into the magma, which cannot expand due to the presence of a sticking plug, resulting in a build up of pressure. Eventually the pressure exceeds the strength of the plug, which fails in stick-slip motion and the pressure is relieved. The magma sticks again when the pressure falls below the dynamic friction value. In this model the time scale of the cycles is controlled by gas diffusion. The influence of permeable gas loss, crystallization and elastic expansion of the conduit on the period of pulsations was studied.

A shorter timescale of order of minutes was investigated in Iverson *et al.* [43] in relation to repetitive seismic events during the 2004-2006 eruption of Mount St. Helens. The flow dynamics is controlled by the presence of a solid plug that is pushed by a Newtonian liquid, with the possibility of a stick-slip transition. Inertia of the plug becomes important on such short timescales.

Models to explain the occurrence of Vulcanian explosions have also been developed by Connor *et al.* [15], Jaquet *et al.* [44] and Clarke *et al*. [13]. A statistical model of repose periods between explosions by Connor *et al.* [15] shows that data fit a log-logistic distribution, consistent with the

interaction of two competing processes that decrease and increase gas pressure respectively. Jaquet *et al.* [44] show the explosion repose period data have a memory. The petrological observations of Clarke *et al*. [13] on clasts from Vulcanian explosions associated with short-term cycles support a model where pressure builds up beneath a plug by gas diffusion, but is opposed by gas leakage through a permeable magma foam. Although these models include some of the key processes and have promising explanatory power, they do not consider the development of the magma plug explicitly. This process is considered in [24], where a model of magma ascent with gas escape is proposed.

V. Long-term cycles.

Figure 3 shows views of three lava domes (Mount St Helens, USA, Santiaguito, Guatemala and Shiveluch, Russia). Measurements of magma discharge rate variations with time are presented below [89, 35, 25]. Behaviour at the first two volcanoes is rather regular, whereas at Shiveluch, long repose periods are followed by an initial rapid increase in eruptive activity with subsequent decrease and complete stop of the eruption. Growth of the lava dome at Unzen volcano, Japan, 1991-1995 was similar to Shiveluch [68, 25].

place figure 3 here

There are three types of conceptual models that attempt to explain long term variation in magma discharge rate. Maeda [53], after [42], considers a simple system that contains a spherical magma chamber located in elastic rocks with a cylindrical conduit located in visco-elastic rocks. Magma viscosity is assumed to be constant. The magma chamber is replenished with a time dependent influx rate. The model reproduces discharge rate variation at Unzen volcano by assuming a bell-shaped form of influx rate dependence on time. There are two controversial assumptions in the model. First, the assumption that the conduit wallrocks are visco-elastic, while the magma chamber wallrocks are purely elastic cannot be justified because near the chamber rock temperature is the highest and it is more reasonable to expect viscous properties for chamber wallrocks rather than for the conduit. The equation that links conduit diameter with magmatic overpressure assumes viscous rock properties up to infinity. If the chamber is located in visco-elastic rocks, oscillations in discharge rate are not possible. Second, in order to obtain reasonable timescales, the rock viscosity must be rather small, of order of 10^{13} Pa s, which is only slightly higher than the typical viscosities of the magma.

Another set of models attribute cyclic behaviour to heat exchange between ascending magma and wallrocks, which accounts for temperature dependent viscosity [95, 17]. The idea of both models is that magma cools down as it ascends, and heat flux is proportional to the difference between the average temperature of the magma and the temperature of the wallrocks. If magma ascends quickly than heat loss is small in comparison with heat advection. Magma viscosity remains low as a consequence and allows high magma discharge rates. In contrast, when magma ascends slowly it can cool substantially and viscosity increases significantly. Both models suggest that, for a fixed chamber pressure, there can be up to three steady state solutions with markedly different discharge rates. Transition between these steady-state solutions leads to cyclic variations in discharge rate. Whitehead and Helfrich [95] demonstrated the existence of cyclic regimes in experiments using corn syrup. In application to magma ascent in a volcanic conduit, these models have strong limitations, because a constant wall-rock temperature is assumed. However, as an eruption progresses the wallrocks heat up and heat flux decreases, a condition that makes periodic behaviour impossible for long-lived eruptions. For such a long-lived eruption like Santiaguito (started in 1922) wallrocks are expected to be nearly equilibrated in temperature with the magma, and heat losses from magma became small. It is possible that this decrease in heat flux contributes to a slow progressive increase in temperature that is observed on timescales longer than the period of pulsations. For example, magma at Santiaguito becomes progressively less viscous, resulting in a transition from mainly lava dome to lava flow activity.

Models, developed by authors of this manuscript, consider that degassing-induced crystallization is a major controlling process for the long-term cyclicity during lava dome building eruptions. There is increasing evidence that there is a good correlation between magma discharge rate and crystallinity of the magma [68, 10]. An increase in crystal content leads to an increase in magma viscosity [16, 20, 21] and, thus, influences magma ascent dynamics. First, we consider a simplified model of magma ascent in a volcanic conduit that accounts for crystallization and rheological stiffening.

V.I. A simplified model

In Barmin *et al*. [3] the following simplifying assumptions have been made in order to develop a semi-analytical approach to magma ascent dynamics.

1. Magma is incompressible. The density change due to bubble formation and melt crystallization is neglected.

2. Magma is a viscous Newtonian fluid. Viscosity is a step function of crystal content. When the concentration of crystals β reaches a critical value β_* the viscosity of magma increases from value μ_1 to a higher value μ_2. Later on we will consider magma rheology in more detail (see Section V.II.II), but a sharp increase in viscosity over a narrow range of crystal content has been confirmed experimentally (e.g., [48, 9].

3. Crystal growth rate is constant and no nucleation occurs in the conduit. The model neglects the fact that magma is a complicated multi-component system and its crystallization is controlled by the degree of undercooling (defined as the difference between actual temperature of the magma and its liquidus temperature). Later in the paper a more elaborate model for magma crystallization will be considered.

4. The conduit is a vertical cylindrical pipe. Elastic deformation of the wallrocks is not included in the model. This assumption is valid for a cylindrical shape of the conduit at typical magmatic overpressures, but is violated when the conduit has a fracture shape. Real geometries of volcanic conduits and their inclination can vary significantly with depth.

5. The magma chamber is located in elastic rocks and is fed from below, with a constant influx rate. For some volcanoes, like Santiaguito or Mount St Helens, average magma discharge rate remained approximately constant during several periods of pulsation. Thus the assumption of constant influx rate is valid. For volcanoes like Mount Unzen or Shiveluch, there is an evidence of pulse-like magma recharge [53, 25].

With above simplification the system of equations for unsteady 1D flow is as follows:

$$\frac{\partial}{\partial t}\rho + \frac{\partial}{\partial x}\rho u = 0;\ \frac{\partial}{\partial t}n + \frac{\partial}{\partial x}nu = 0; \qquad \text{(1a)}$$

$$\frac{\partial p}{\partial x} = -\rho g - \frac{32\mu u}{\delta^2};\quad \mu = \begin{cases}\mu_1, & \beta < \beta_* \\ \mu_2, & \beta \geq \beta_*\end{cases} \qquad \text{(1b)}$$

$$\frac{\partial}{\partial t}\beta + u\frac{\partial \beta}{\partial x} = 4\pi n r^2 \chi = \left(36\pi n\right)^{1/3}\beta^{2/3}\chi \qquad \text{(1c)}$$

Here ρ is the density of magma, u is the vertical cross-section averaged ascent velocity, n is the number density of crystals per unit volume, p is the pressure, g is the acceleration due to gravity, δ is the conduit diameter, β is the volume concentration of crystals, β_* is a critical concentration of crystals above which the viscosity changes from μ_1 to μ_2, r is the crystal radii, χ is the linear crystal growth rate, and x is the vertical coordinate. The first two equations (1a) represent the conservation of mass and the number density of crystals, the second (1b) is the momentum equation with negligible inertia, and the third (1c) is the crystal growth equations with χ = constant. We assume the following boundary conditions for the system (1):

$$x = 0: \frac{dp_{ch}}{dt} = \frac{\gamma}{V_{ch}}\left(Q_{in} - Q_{out}\right);\ \beta = \beta_{ch};\ n = n_{ch}$$

$$x = l: p = 0$$

Here γ is the rigidity of the wall-rock of the magma chamber, V_{ch} is the chamber volume, β_{ch} and n_{ch} are the crystal concentration and number density of crystals per unit volume in the chamber, p_{ch} is the pressure in the chamber, l is the conduit length, Q_{in} is the flux into the chamber and $Q_{out} = \pi \delta^2 u/4$ is the flux out of the chamber into the conduit. Both β_{ch} and n_{ch} are assumed constant. We neglect the influence of variations of the height of the lava dome on the pressure at the top of the conduit and assume that the pressure there is constant. As the magma is assumed to be

incompressible, the pressure at the top of the conduit can be set to zero because the atmospheric pressure is much smaller than magma chamber pressure.

From the mass conservation equation for the case of constant magma density, $u = u(t)$ and $n = n_{ch}$ everywhere. Equations (1) can be integrated and transformed from partial differential equations to a set of ordinary differential equations with state-dependent delay representing a "memory" effect on crystal concentration (see [3] for details).

V.I.I. Results and applications

The general steady-state solution for magma ascent velocity variations with chamber pressure is shown in Figure 4a. Solutions at high magma ascent velocities, when the critical concentration of crystals is not reached inside the conduit, result in a straight line (CB), which is the same as for the classical Poiseuille solution for a fluid with constant viscosity. At low ascent velocities there is a quadratic relationship (OAC) between chamber pressure and ascent velocity (see [3] for derivation of the equation). A key feature of the steady-state solution is that, for a fixed chamber pressure, it is possible to have three different magma ascent velocities. We note that for $\mu_2/\mu_1 = 1$ only the branch CB exists and for $1 < \mu_2/\mu_1 \leq 2$ there is a smooth transition between the lower branch (ODA) and the upper branch (CB) and multiple steady-state regimes do not exist.

place figure 4 here

We first consider the case where chamber pressure changes quasi-statically and the value of Q_{in} is between Q_A and Q_C. Starting at point O the chamber pressure increases, because the influx into the chamber is higher than the outflux. At point A, a further increase in pressure is not possible along the same branch of the steady-state solution and the system must change to point B, where the outflux of magma is larger than the influx. The chamber pressure and ascent velocity decrease along BC until the point C is reached and the system must change to point D. The cycle DABC then repeats itself. Provided the chamber continues to be supplied at the same constant rate repetition of this cycle results in periodic behaviour. The transitions AB and CD in a cycle must involve unsteady flow.

Oscillations in magma discharge rate involve large variations in magma crystal content. This relation is observed on many volcanoes. For example, pumice and samples of the Soufrière Hills dome that were erupted during periods of high discharge [88] have high glass contents (25 to 35%) and few microlites [65], whereas samples derived from parts of the dome that were extruded more slowly (days to weeks typically) have much lower glass contents (5 to 15%) and high contents of groundmass microlites. These and other observations [68, 34] suggest that microlite crystallization can take place on similar time scales to the ascent time of the magma

Of more general interest is to consider unsteady flow behaviour. We assume that the initial distribution of parameters in the conduit corresponds to the steady-state solution of system (1) with the initial magma discharge rate, Q_0, being in the lowest regime. The behaviour of an eruption with time depends strongly on the value of Q_{in}. If Q_{in} corresponds to the upper or the lower branch of the steady state solution the eruption stabilises with time with $Q = Q_{in}$ and $dp_{ch}/dt = 0$. However, if Q_{in} corresponds to the intermediate branch of the steady-state solution, with Q_{in} between Q_A and Q_C, periodic behaviour is possible. Figure 4b shows three eruption scenarios for different values of the magma chamber volume V_{ch}. When V_{ch} is small the eruption stabilizes with time. In contrast, undamped periodic oscillations occur for values of V_{ch} larger than some critical value. For very large magma chamber volumes the transient solution almost exactly follows the steady-state solution, with unsteady transitions between the regimes. The time that the system spends in unsteady transitions in this case is much shorter than the period of pulsations. The maximum discharge rate during the cycle is close to Q_B, the minimum is close to Q_D and the average is equal to Q_{in}. The period of pulsations increases as the volume of magma chamber increases.

Now we apply the model to two well-documented eruptions: the growth of lava domes on Mount St. Helens (1980-1986) and on Santiaguito (1922-present). Our objective here is to establish that the model can reproduce the periodic behaviours observed at these two volcanoes. Estimates can be obtained for most of the system parameters. However, magma chamber size is not well-constrained and so the model can be used to make qualitative inferences on relative chamber size. Given the uncertainties in the parameter values and the simplifications in the model development, the

approach can be characterized as mimicry. Adjustments in some parameters were made to achieve best fits with observations, but the particular best-fits are not unique.

For Mount St. Helens our model is based on data presented by [89]. Three periods of activity can be distinguished during the period of dome growth. The first period consists of 9 pulses of activity with average peak magma discharge rates ~ 15 m^3/s during 1981-1982. Each pulse lasted from 2 to 7 days (with a mean value of 4 days) with the average period between the pulses being 74 days and the average discharge rate during the period being Q_1 ~ 0.67 m^3/s. The second period is represented by continuous dome growth and lasted more than a year (368 days) with a mean magma discharge rate of Q_2 ~ 0.48 m^3/s. During the last period there were 5 episodes of dome growth with peak magma discharge rates up to ~ 15 m^3/s, an average period of pulsation of ~ 230 days and a mean discharge rate of Q_3 ~ 0.23 m^3/s. We assume that the intensity of influx into the magma chamber, Q_{in}, is equal to the average magma discharge rate over the corresponding periods. There might have been a progressive decrease in the intensity of influx during the eruption, but, due to limitations of the model, we assume that Q_{in} changes as a step function between the periods.

place figure 5 here

The best-fit model for the eruption is presented in Figure 5a, with the parameters used for the simulation summarized in Table 2 in [3]. During the first period of the eruption $Q_{in} = Q_1$. This corresponds to the intermediate branch of the steady-state solution and cyclic behaviour occurs. In the second period $Q_{in} = Q_2$ the system moves to the lower regime and the eruption stabilizes with time. For the third period of the eruption the parameters of the system have been changed, so that $Q_{in} = Q_3 < Q_2$, corresponding to the intermediate regime once again and periodic behaviour occurs. This condition can be satisfied by a decrease in the diameter of the conduit, or a decrease in crystal growth rate, or the number density of crystals. All these mechanisms are possible: decrease in the diameter could be a consequence of magma crystallization on the conduit walls, while a decrease in either crystal growth rate or number density of crystals could be reflect observed changes in magma composition [89]. The influence of conduit diameter is the strongest because ascent velocity, for the same discharge rate, depends on the square of the diameter. The required change in diameter is from 18 to 12 m, but this change can be smaller if we assume a simultaneous decrease in crystal growth rate.

Since 1922, lava extrusion at Santiaguito has been cyclic [35]. Each cycle begins with a 3-6 year long high (0.5-2.1 m^3/s) magma discharge rate phase, followed by a longer (3-11 years) low (~ 0.2 m^3/s) discharge rate phase. The time-averaged magma discharge rate was almost constant at ~0.44 m^3/s between 1922 and 2000. The first peak in discharge rate had a value >2 m^3/s, whereas the second peak had a much smaller value. The value for the second peak is underestimated as it is calculated based on the dome volume only, but does not include the volume of dome collapse pyroclastic flows. Later peaks show an increase in magma discharge rate until 1960 (Figure 5b, dashed line). Post-1960, the duration of the low discharge rate phase increased, the peak discharge and the time-averaged discharge rates for each cycle decreased, and the difference between discharge rates during the high and low discharge rate phases of each cycle decreased. Our best-fit model is shown in Figure 5b and the parameters estimates are listed in Table 2 in [3]. The model reproduces the main features of the eruption, including the period of pulsations, the ratio between low and high magma discharge rates, and the range of observed discharge rates. We cannot, however, reproduce the decrease in the amplitude of pulsations within the framework of the model using fixed parameter values.

The theory provides a potential method to estimate magma chamber volumes. For Mount St Helens our estimate of the chamber size (~ 0.6 km^3) is comparable with the total erupted volume in the entire 1980-86 eruption and is consistent with the fact that geophysical imaging did not identify a large magma body. Santiaguito volcano erupted more than 10 km^3 in the 1902 explosive eruption [96] and more than 1 km^3 of lava domes since 1922. The best-fit model estimate of a large (64 km^3) chamber is consistent with much larger eruption volumes, long periods, and longevity of the eruption in comparison to Mount St Helens. One limitation of the model is that the supply of deep magma from depth to the chamber is assumed to be constant.

V.II. Model development

In this section we further develop models to examine new effects and relax some of the simplifications of earlier models. We investigate a number of effects that were not fully explained or

considered in previous studies [61, 62, 3]. The new model incorporates a more advanced treatment of crystallization kinetics based on the theoretical concepts developed in [46, 38], and is calibrated by experimental studies in andesitic systems [22, 34]. In particular, we distinguish growth of phenocrysts formed in the magma chamber from crystallization of microlites during magma ascent. Previous models have assumed that magma is always Newtonian, so we study models of conduit flow assuming non-Newtonian rheology, with rheological properties being related to crystal content. Latent heat is released during the crystallization of ascending magma due to degassing and we show that this can have an important influence on the dynamics. Elastic deformation of conduit walls leads to coupling between magma ascend and volcano deformations.

V.II.I. System of equations

We model magma ascent in a dyke-shaped conduit with elliptical cross-section using a set of 1D transient equations written for horizontally averaged variables [20, 21]:

$$\frac{1}{S}\frac{\partial}{\partial t}(S\rho_m) + \frac{1}{S}\frac{\partial}{\partial x}(S\rho_m V) = -G_{mc} - G_{ph} \tag{2}$$

$$\frac{1}{S}\frac{\partial}{\partial t}(S\rho_{mc}) + \frac{1}{S}\frac{\partial}{\partial x}(S\rho_{mc} V) = G_{mc} \tag{3a}$$

$$\frac{1}{S}\frac{\partial}{\partial t}(S\rho_{ph}) + \frac{1}{S}\frac{\partial}{\partial x}(S\rho_{ph} V) = G_{ph} \tag{3b}$$

$$\frac{1}{S}\frac{\partial}{\partial t}(S\rho_d) + \frac{1}{S}\frac{\partial}{\partial x}(S\rho_d V) = -J \tag{4a}$$

$$\frac{1}{S}\frac{\partial}{\partial t}(S\rho_g) + \frac{1}{S}\frac{\partial}{\partial x}(S\rho_g V_g) = J \tag{4b}$$

Here t denotes time, x the vertical coordinate, ρ_m, ρ_{ph}, ρ_{mc}, ρ_d and ρ_g are the densities of melt, phenocrysts, microlites, dissolved gas and exsolved gas respectively, and V and V_g are the velocities of magma and gas, respectively. G_{ph}, G_{mc} represent the mass transfer rate due to crystallization of phenocrysts and microlites, respectively, and J the mass transfer rate due to gas exsolution, S is the cross-section area of the conduit. Eq. (2) represents the mass conservation for the melt phase, eqs. (3a) and (3b) are the conservation equations for microlites and phenocrysts respectively, eqs. (4a) and (4b) represent the conservation of the dissolved gas and of the exsolved gas respectively.

$$\frac{\partial p}{\partial x} = -\rho g - F_c \tag{5}$$

$$V_g - V = -\frac{k}{\mu_g}\frac{\partial p}{\partial x} \tag{6}$$

Here p is the pressure, ρ the bulk density of magma, g the acceleration due to gravity, μ is the magma viscosity, k is the magma permeability and μ_g is the gas viscosity. Eq. (5) represents the equation of momentum for the mixture as a whole, in which the pressure drops due to gravity and conduit resistance are calculated for laminar flow in an elliptic pipe. Eq. (6) is the Darcy law for the exsolved gas flux through the magma.

$$\frac{1}{S}\frac{\partial}{\partial t}(S\rho C_m T) + \frac{1}{S}\frac{\partial}{\partial x}(S\rho C_m V T) = L_*(G_{mc} + G_{ph}) - C_m T J - Q_{cl} + Q_{vh} \tag{7}$$

Here C_m is the bulk specific heat of magma, T is the bulk flow-averaged temperature, L_* is latent heat of crystallization, Q_{cl} denotes the total heat loss by conduction to the conduit walls, and Q_{vh} denotes the total heat generation due to viscous dissipation. Here we consider the case of the latent heat release. This assumption is valid when both $Q_{cl} \approx 0$ and $Q_{vh} \approx 0$ or when $Q_{cl} + Q_{vh} \approx 0$. The study of

the effects of both heat loss and viscous heating, which are intrinsically two-dimensional [18, 19], and their parameterization is the subject of ongoing research.

$$\rho_m = \rho_m^0(1-\alpha)(1-\beta)(1-c) \quad ; \ \rho_c = \rho_c^0(1-\alpha)\beta \tag{8a}$$

$$\rho_d = \rho_m^0(1-\alpha)(1-\beta)c \, ; \ \rho_g = \rho_g^0\alpha \tag{8b}$$

$$\rho = \rho_m + \rho_c + \rho_d + \rho_g \tag{8c}$$

$$\alpha = \frac{4}{3}\pi r_b^3 n; \ \ \frac{\partial}{\partial t}(Sn) + \frac{\partial}{\partial x}(SnV) = 0; \ \ p = \rho_g^0 RT \tag{9}$$

Here α is the volume concentration of bubble, β is the volume concentration of crystals in the condensed phase (melt plus crystals), and c is mass concentration of dissolved gas (equal to volume concentration as we assume that the density of dissolved volatiles is the same as the density of the melt), ρ_0^m denotes the mean density of the pure melt phase, ρ_0^c is density of the pure crystal phase (with $\rho_c = \rho_{ph} + \rho_{mc}, \beta = \beta_{ph} + \beta_{mc}$), r_b is the bubble radius, and n the number density of bubble per unit volume. Concerning the parameterization of mass transfer rate functions, we use:

$$J = 4\pi r_b n D \rho_m^0 \left(c - C_f\sqrt{p}\right) \tag{10}$$

$$G_{mc} = 4\pi\rho_c^0(1-\beta)(1-\alpha)U(t)\int_0^t I(\omega)\left(\int_\omega^t U(\eta)d\eta\right)^2 d\omega \tag{11a}$$

$$G_{ph} = 3\gamma_s\left(\frac{4\pi N_{ph}\beta_{ph}^2}{3}\right)^{1/3}\rho_c^0(1-\beta)(1-\alpha)U(t) \tag{11b}$$

Here J is parameterized using the analytical solution described in [69], U is the linear crystal growth rate ($\mathrm{m\,s^{-1}}$), I is the nucleation rate ($\mathrm{m^{-3}s^{-1}}$), which defines the number of newly nucleated crystal per cubic meter, and γ_s is a shape factor of the order of unity, D and C_f are the diffusion and the solubility coefficients, respectively. Concerning the mass transfer due to crystallization G_{mc}, we adapt a model similar to that described in [38]. Assuming spherical crystals, the Avrami-Johnson-Mehl-Kolmogorov equation in the form adopted by [46], for the crystal volume increase rate, is:

$$\frac{d\beta}{dt} = 4\pi \mathrm{Y}_t U(t)\int_0^t I(\omega)\left(\int_\omega^t U(\eta)d\eta\right)^2 d\omega$$

where $\mathrm{Y}_t = (1-\beta)(1-\alpha)$ is the volume fraction of melt remaining uncrystallized at the time t. Therefore, we have $G_{mc} = \rho_{mc}\, d\beta/dt$. For the phenocryst growth rate G_{ph} we assume that it is proportional to the phenocryst volume increase rate $d\beta_{ph}/dt = 4\pi R_{ph}^2 N_{ph} U(t)$ times the crystal density ρ_c^0 times the volume fraction of melt remaining uncrystallized at the time t. A detailed description of the parameterization used for the different terms is reported in [63].

For parameterizations of magma permeability k and magma viscosity μ we use:

$$k = k(\alpha) = k_0\alpha^j \tag{12}$$

$$\mu = \mu_m(c,T)\theta(\beta)\eta(\alpha,Ca) \tag{13}$$

where k is assumed to depend only on bubble volume fraction α. Magma viscosity μ depends on water content, temperature, crystal content, bubble fraction and capillary number as described in detail in the next section.

Regarding equations for semi-axes, a and b, we assume that the elliptical shape is maintained and that pressure change gradually in respect with vertical coordinate and time so that the plain strain analytical solution for an ellipse subjected to a constant internal overpressure [64, 66], remains valid:

$$a = a_0 + \frac{\Delta P}{2G}\left[-(1-2\nu)a_0 + 2(1-\nu)b_0\right] \qquad (14a)$$

$$b = b_0 + \frac{\Delta P}{2G}\left[2(1-\nu)a_0 - (1-2\nu)b_0\right] \qquad (14b)$$

where ΔP is the overpressure, i.e. the difference between conduit pressure and far field pressure (here assumed to be lithostatic for a sake of simplicity), a_0 and b_0 are the initial values of the semi-axes, ν is the host rock Poisson ratio, and G is the host rock rigidity.

Eqs. (2)-(14) are solved between the top of the magma chamber and the bottom of the lava dome that provides some constant load by using the numerical method described in [63]. The effects of dome height and morphology changes are not considered in this paper. We consider three different kinds of boundary conditions at the inlet of the dyke: constant pressure, constant influx rate and the presence of a magma chamber located in elastic rocks. The case of constant pressure is applicable when a dyke starts from either a large magma chamber or unspecified source, so that pressure variations in the source region remain small. An estimate of the volume of magma stored in the source region that allows pressure to be approximated as constant depends on wall-rock elasticity, magma compressibility (volatile content), and the total volume of the erupted material. If the magma flow at depth is controlled by regional tectonics, the case of constant influx rate into the dyke may be applicable if total variations in supply rate are relatively small on the timescale of the eruption.

For the case where magma is stored in a shallow magma chamber prior to eruption, and significant chamber replenishment occurs, the flow inside the conduit must be coupled with the model for the magma chamber. In this case, as explained in detail in [63], we assume that the relationship between the pressure at the top of the magma chamber p_{ch} and the intensity of influx Q_{in} and outflux Q_{out} of magma to and from the chamber is given by:

$$\frac{dp_{ch}}{dt} = \frac{4G\langle K\rangle}{\langle\rho\rangle V_{ch}\left(3\langle K\rangle + 4G\right)}\left(Q_{in} - Q_{out}\right) \qquad (15)$$

where V_{ch} is the magma chamber volume, $\langle\rho\rangle$ and $\langle K\rangle$ are the average magma density and magma bulk modulus, respectively, and G is the rigidity of rocks surrounding the chamber.

Cases of constant influx and of constant source pressure are the limit cases of equation (15) in the case of infinitely small and infinitely large magma chamber volume. We assume that the volume concentration of bubbles and phenocrysts are determined by equilibrium conditions and that the temperature of the magma is constant. The effect of temperature change on eruption dynamics, due to interaction between silicic and basaltic magma, was studied in [63].

We use a steady-state distribution of parameters along the conduit as an initial condition for the transient simulation. The values are calculated for a low magma discharge rate, but the particular value of this parameter is not important because the system deviates from initial conditions to a cyclic or stabilized state, which does not depends on the initial conditions.

V.II.II. Rheology of crystal-bearing magma and conduit resistance

Magma viscosity is modelled as a product of melt viscosity $\mu_m(c, T)$, the relative viscosity due to crystal content $\theta(\beta) = \Theta(\beta)\varphi(\beta)$, and the relative viscosity due to the presence of bubbles $\eta(\alpha, Ca)$. The viscosity of the pure melt $\mu_m(c, T)$ is calculated according to [36]. Viscosity increase due to the presence of the crystals is described through the function $\Theta(\beta)$ [16, 20, 21]. As crystallization proceeds, the remaining melt becomes enriched in silica- and melt viscosity increases. The

parameterization of this effect is described by the function $\varphi(\beta)$ in [25, 21]. Effects of the solid fraction are parameterized as described in [21].

Effects due to the presence of bubbles are accounted for by adopting a generalization of [51] for an elliptical conduit [20, 21].

In the case of Newtonian magma rheology, the friction force in an elliptical conduit can be obtained from a classical Poiseuille solution for low Reynolds number flow $F_c = 4\mu\frac{a^2+b^2}{a^2b^2}V$ [47]. High crystal or bubble content magmas may show non-Newtonian rheology. One possible non-Newtonian rheology is that of a Bingham material characterized by a yield strength τ_b [4]. The stress-strain relation for this material is given by:

$$\tau_{ij} = \left(\mu + \frac{\tau_b}{\gamma}\right)\gamma_{ij} \Leftrightarrow \tau > \tau_b \qquad (16)$$

$$\gamma_{ij} = 0 \Leftrightarrow \tau \le \tau_b$$

Here τ_{ij} and γ_{ij} are the stress and strain rate tensors, τ and γ are second invariants of corresponding tensors. According to this rheological law, the material behaves linearly when the applied stress is higher than a yield strength. No motion occurs if the stress is lower than a yield strength. In the case of a cylindrical conduit the average velocity can be calculated in terms of the stress on the conduit wall τ_w [52]:

$$V = \frac{1}{12}\frac{r}{\tau_w^3\mu}\left(\tau_b^4 + 3\tau_w^4 - 4\tau_b\tau_w^3\right) \qquad (17)$$

Here r is the conduit radii. This form of equation gives an implicit relation between ascent velocity and pressure drop, and is not convenient to use. By introducing dimensionless variables $\Pi = \mu V/\tau_b r$ and $\Theta = \tau_w/\tau_b \ge 1$ relation (17) can be transformed into:

$$\Theta^4 - \frac{1}{6}(8+3\Pi)\Theta^3 + \frac{1}{3} = 0 \qquad (18)$$

Following [63] a semi-analytical solution can be used for (18) and the conduit friction force can be expressed finally as: ___ _____. We note that a finite pressure gradient is necessary to initiate the flow in the case of Bingham liquid, in contrast to a Newtonian liquid.

VI.I.I. Results and applications

Influence of non-Newtonian properties on eruption behaviour.

Now we compare the dynamics of magma extrusion in the cases of Newtonian and Bingham rheology. We will assume that yield strength is reached when the concentration of crystals reaches a critical value:

$$\tau = \begin{cases} \tau_b \text{ for } \beta > \beta_{cr} \\ 0 \quad \text{for } \beta \le \beta_{cr} \end{cases} \qquad (19)$$

Fig 6a shows a set of steady-state solutions for different values of τ_b. Values of τ_b and β_{cr} depend on crystal shape, crystal size distribution, magma temperature and other properties, but here are assumed to be constant. To illustrate the influence of Bingham rheology, the value of $\beta_{cr} = 0.65$ was chosen so that, for discharge rate larger then ~ 5 m^3/s, the magma has Newtonian rheology (see Fig 6a). A more detailed study would require measurements of the rheological properties of magma for a wide range of crystal content and crystal size distributions. As the value of τ_b the chamber pressure that is necessary to start the eruption increases.

place figure 6 here

Fig. 6b shows the influence of these two rheological models on the dynamics of magma extrusion. In the case of Bingham rheology, magma discharge rate between the two pulses is zero until a critical chamber overpressure is reached. Then the magma discharge rate increases rapidly with decrease in crystal content, leading to a significant reduction of both magma viscosity and the length of the part of the conduit that is occupied by the Bingham liquid where $\beta_c > \beta_{cr}$ .There is a transition in the system to the uppermost flow regime and the pressure then decreases quickly. Because the pressure at the onset of the pulse was significantly larger than in the case of a Newtonian liquid, the resulting discharge rate in the case of Bingham rheology is also significantly higher.

Modelling of conduit flow during dome extrusion on Shiveluch volcano

The maximum intensity of extrusion was reached at an early stage in all three eruptions (Figure 3). We therefore suggest that dome extrusion was initiated by high overpressure in the magma chamber with respect to the lithostatic pressure. Depressurization of the magma chamber occurred as a result of extrusion. Without magma chamber replenishment, depressurization results in a decrease in magma discharge rate. In open system chambers replenishment of the chamber during eruption can lead to pulsatory behaviour [3]. The following account is derived from [25]. For the 1980-1981 eruption the monotonic decrease in discharge rate indicates that there was little or no replenishment of the magma chamber. During the 1993-1995 and 2001-2004 episodes, however, the magma discharge rate fluctuated markedly, suggesting that replenishment was occurring. The influx of new magma causes an increase in magma chamber pressure, and a subsequent increase in magma discharge rate. During the 2001-2004 eruption there were at least three peaks in discharge rate. Replenishment of the magma chamber with new hot magma can explain the transition from lava dome extrusion to viscous lava flow that occurred on Shiveluch after 10 May 2004, and which continues at the time of writing (2007).

place figure 7 here

We simulated dome growth during the 2001-2002, because this dataset is the most complete and is supported by petrological investigations [39]. We assume the shape of the influx curve:

$$Q_{in} = \begin{cases} 0, t < t_s \\ Q_0, t_s \le t \le t_f \\ 0, t > t_f \end{cases} \qquad (20)$$

Influx occurs with constant intensity Q_0 between times t_s and t_f. We have examined many combinations of values of these parameters within the constraints provided by observations. The best simulation results use the following values of parameters: Q_0 = 3.8 m^3/s, t_s = 77 and t_f = 240 days. A more continuous influx, dependent on time, is plausible, but there is no geophysical evidence that allows us to constrain the intensity of the influx, because ground deformation data are absent for Shiveluch volcano. The output of the model gives a magma chamber volume of 12 km^3, assuming a spherical chamber. Figure 7a shows the time-dependence of magma discharge rate, and Fig. 7b shows the increase in the volume of erupted material with time after 6th June 2001. The timing of magma influx is in good agreement with the residence time of basaltic magma in the system, as calculated from the olivine reaction rims. For further details see [25].

5 to 7 weeks cycles on the Soufriere Hills Volcano: evidence for a dyke?

An approximately 5 to 7 week cyclic pattern of activity was recognized at the Soufrière Hills Volcano (SHV) [91, 87] between April 1997 and March 1998 from peaks in the intensity of eruptive activity and geophysical data, including tilt and seismicity (Figure 2).

In models discussed above, the time-scale of pulsations depends principally on the volume of the magma chamber, magma rheology and the cross-sectional area of the conduit. These models might provide an explanation for the 2-3 year cycles of dome extrusion observed at SHV, where

deformation data indicate that the magma chamber regulates the cycles. However, the models cannot simultaneously explain the 5-7 week cycles. Thus another mechanism is needed.

The evidence for a dyke feeder at SHV includes GPS data [58], distribution of active vents, and seismic data [76]. We have assumed that, at dept, the conduit has an elliptical shape that transforms to a cylinder at shallow level. In order to get a smooth transition from the dyke at depth to a cylindrical conduit (see Figure 1) the value of a_0 in equations (14) is parameterized as:

$$a_0(x) = A_1 \arctan\left(\frac{x - L_T}{w_T}\right) + A_2 \qquad (21)$$

Here L_T and w_T are the position and the vertical extent of the transition zone between the ellipse and the cylinder and constants A_1 and A_2 are calculated to satisfy conditions $a_0(L) = R$ and $a_0(0) = a_0$, where R is the radius of the cylindrical part of the conduit and a_0 is the length of semi-major axis at the inlet of the dyke. The value of b_0 is calculated in order to conserve the cross-section area of the unpressurized dyke, although it can also be specified independently.

In order to de-couple the influence of the dyke geometry from the oscillations caused by magma chamber pressure variations, we have assumed a fixed chamber pressure as a boundary condition for the entrance to the conduit. This assumption is valid because the timescale of chamber pressure variations are much longer than the period of the cycle (2-3 years in comparison with 5-7 weeks).

place figure 8 here

Results presented in Figure 8 show that, even with a fixed chamber pressure, there are magma discharge rate oscillations. At the beginning of a cycle the magma discharge rate is at a minimum, while the overpressure (here presented for 1 km depth by a dashed line) and dyke width are at a maximum. At point A in Figure 8a the crystal content and viscosity have reached their maximum values. Beyond this threshold condition, an increase in magma discharge rate results in decreasing pressure and dyke width. However, crystal content and viscosity also decrease and this effect decreases friction, resulting in flow rate increase and pressure decrease. At C the system reaches minimum viscosity and crystal content, which cannot decline further. Thereafter the magma discharge rate decreases, while the pressure and dyke width increase. The dyke acts like a capacitor, storing volume during this part of the cycle.

The period of oscillation depends on several parameters such as influx rate and dyke aspect ratio a/R. Typically the period decreases with increasing aspect ratio. The range of calculated periods varies between 38 and 51 days for semi major-axis lengths, a, from 175 to 250 m and semi minor-axes, b, from 2 to 4 m. These results match observed cyclicity at SHV. The start of a cycle is quite sharp (Fig. 2), with the onset of shallow hybrid-type (impulsive, low-frequency coda) earthquakes. The change to shorter period and higher amplitude tilt pulsations indicate a marked increase in average magma discharge rate [91, 98]. The model cycles also have rapid onsets. The high-amplitude tilt pulsations lasted for several weeks [91], consistent with the duration of higher magma discharge rates early in each 5-7 week cycle. Tilt data (Fig. 2) are consistent with the model in that the episode of high magma discharge is associated with a marked deflation that lasts several weeks (see dashed curve at Fig. 8, representing magmatic overpressure at 1 km depth). The magma pressure builds up in the swelling dyke and then reaches a threshold, whereupon a surge of partly crystallized magma occurs, accompanied by elevated seismicity.

The models presented above have certain general features that are necessary to show cyclic behaviour. First of all, the resistance of the conduit must depend on magma discharge rate in a way that resistance decreases when discharge rate increases in some range of discharge rate. This dependence is reproduced by a sigmoidal curve. Resistance is a product of viscosity and velocity, and is linearly proportional to discharge rate. This means that magma viscosity must decrease as discharge rate strongly increases. There may be many reasons for this behaviour, including crystallization, temperature variation or gas diffusion. The second condition is that there must be some capacitor in the system that can store magma in a period of low discharge rate and release it in a period of high discharge rate. The role of this capacitor can be played by a magma chamber or dyke-shaped conduit located in elastic rocks, or by compressibility of the magma itself. The volumes of these capacitors are different and thus will cause pulsations with different periods. Currently there is no single model that can account for pulsations with multiple timescales.

VII. Future Directions

Our models indicate that magmatic systems in lava dome eruptions can be very sensitive to small changes in parameters. This sensitivity is most marked when the system is close to the cusps of steady-state solutions. If magma discharge rate becomes so high that gas cannot escape efficiently during magma ascent, then conditions for magma fragmentation and explosive eruption can arise. Empirical evidence suggests that conditions for explosive eruption arise when magma discharge rates reach approximately 10 m^3/s or more in dome eruptions [45, 83]. Calculations show the possibility of such high discharge rates for the system parameters typical of lava dome-building eruptions.

We have illustrated model sensitivity of results by varying only one parameter at a time on plots of chamber pressure and discharge rate. However, magmatic systems have many controlling parameters that may vary simultaneously. Furthermore, some controlling parameters are likely to be interdependent (such as temperature, volatile content and phenocryst content, for example) and others may be independent (such as magma temperature and conduit dimensions). An eruption can be expected to move through n-parameter space, making simulation and its parameter depiction difficult. Our results are simplified, so system sensitivity and behaviour in the real world may be yet more complex. A volcanic system may be quite predictable when it is within a stable regime, but may become inherently unpredictable [84, 85] when variations in the parameters move the system towards transition points and flow regime boundaries.

As in all complex systems there are many controlling parameters. Our models capture some of the key dynamics, but are still simplified in many respects, so do not fully capture the real variations. Our models do not, for example, consider variations in dome height, gas escape to surrounding rocks, strain-rate dependent rheological effects or time dependent changes in conduit diameter. The model for porosity is based on interpretation of measurements of porosity of erupted magma. The role of post-eruptive alterations of pore structure, for example, formation of cooling cracks, cannot be easily estimated. The model of bubble coalescence and permeability formation is important for understanding gas escape mechanisms and will provide constraints on transitions between extrusive and explosive activity. Because the model remains 1D, lateral distribution of parameters cannot be studied. These includes: lateral pressure gradients, magma crystallization on the conduit walls, wallrocks melting or erosion, formation of shear zones and shear heating, heat flux to surrounding rocks. The models also make the simplifying assumption that influx into the chamber from a deep source is a constant, or given as a function of time. The dynamics of the magma chamber itself are oversimplified in all existing conduit flow models. Changes in magma properties in magma chamber can affect the long-term evolution of eruptions. We have considered water as the only volatile and the addition of other gas species (e.g. CO_2 and SO_2) would add further variability.

There are large uncertainties in some parameters, which are likely to be very strong controls, such as the rheological properties of high crystalline magmas and crystal growth kinetic parameters, notably at low pressures (<30 MPa) where experiments are very difficult to do (e.g. [22]). More experiments are necessary to understand the rheology of multiphase systems containing melt, crystals and bubbles. The effects of crystal shape, crystal size distribution and strain rate remain largely unclear. Some parameters, such as conduit geometry variation with depth, are highly uncertain. With so many parameters, good fits can be achieved by selecting plausible values for real systems. Barmin *et al.* [3], for example, were able to reproduce the patterns of discharge rate at Mount St Helens and Santiaguito quite accurately. However, such models are not unique, partly because the actual values of some parameters may be quite different to the assumed values and partly because of the model simplifications.

Results obtained from waveform inversions of very-long-period seismic data over the past few years point to the predominance of a crack-like geometry for volcanic conduits [11], and it is becoming increasingly evident that the details of this geometry, such as conduit inclination, a sudden change in conduit direction, a conduit bifurcation, or a sudden increase in cross section, are all critically important in controlling magma flow dynamics. Future modelling attempts will need to be closely tied to information on conduit geometry derived from seismology to provide a more realistic view of volcanic processes.

The full simulation of any particular volcanic eruption in such a non-linear and sensitive system may appear a hopeless task. However, some reduction in uncertainties will certainly help to make the models more realistic. Further experimental studies of crystallization kinetics and the rheological properties of magma at high crystallinities are among the most obvious topics for future research.

Advances in understanding the controls on magma input into an open-system chamber would be beneficial, since the delicate balance between input and output is a prime control on periodic behaviour.

Further model development includes 2D effects, elastic deformation effects in dyke-fed domes and coupling between magma chamber and conduit flow dynamics. Even with such improvements, large parameter uncertainties and modelling difficulties will remain. In such circumstances the logical approach is to start quantifying the uncertainties and sampling from them to produce probabilistic outputs based on ensemble models where numerical models of the kind discussed here can be run many times. A future challenge for numerical models will also be to produce simulated outputs which compare in detail with observations, in particular time series of magma discharge rates.

Acknowledgements This work was supported by NERC research grant reference NE/C509958/1. OM and AB acknowledges Russian Foundation for Basic Research (05-01-00228) and President of Russian Federation program (NCH-4710.2006.1). RSJS acknowledges a Royal Society Wolfson Merit Award. The Royal Scoiety exchange grants and NERC grants had supported the Bristol/Moscow work over the last 10 years.

VIII. Bibliography

Primary Literature

1. Balmforth NJ, Burbidge AS, Craster RV (2001) Shallow Lava Theory. In Balmforth NJ, Provenzale A (eds) Geomorphological Fluid Mechanics, Lecture Notes in Physics, Vol 582, pp 164-187
2. Balmforth NJ, Burbidge AS, Craster RV, Rust AC, Sassi R (2006) Viscoplastic flow over an inclined surface, J Non-Newtonian Fluid Mech, Vol 139, pp 103–127
3. Barmin A, Melnik O, Sparks RSJ (2002) Periodic behaviour in lava dome eruptions. Earth Planet Sc Lett, Vol 199, pp 173-184
4. Bingham EC (1922) Fluidity and Plasticity, 215 pp, McGraw-Hill, New York
5. Blake S (1990) Viscoplastic models of lava domes. In: Fink JH (ed) Lava flows and domes, Vol 2. In: Fink JH (ed) Lava flows and domes; emplacement mechanisms and hazard implications. Springer Verlag, Berlin, pp 88-126
6. Blundy JD, Cashman KV, Humphreys MCS (2006) Magma heating by decompression-driven crystallisation beneath andesite volcanoes, Nature, Vol 443, pp 76-80, doi:10.1038/nature05100
7. Calder, E. S., Luckett, R. Sparks, R. S. J. & Voight, B. 2002. Mechanisms of lava dome instability and generation of rockfalls and pyroclastic flows at Soufrière Hills Volcano, Montserrat. In: Druitt, T. H. & Kokelaar, B. P. (eds) The Eruption of Soufrière Hills Volcano, Montserrat, from 1995 to 1999, Geological Society, London, Memoirs, 21, 173–190
8. Calder E. S., J. A. Cortés, J. L. Palma, R. Luckett (2005), Probabilistic analysis of rockfall frequencies during an andesite lava dome eruption: The Soufrière Hills Volcano, Montserrat, Geophys. Res. Lett., 32, L16309, doi:10.1029/2005GL023594
9. Caricchi L, Burlini L, Ulmer P, Gerya T, Vassalli M, Papale P (2007) Non-Newtonian rheology of crystal-bearing magmas and implications for magma ascent dynamics. Earth Planet Sc Lett, in press
10. Cashman KV, Blundy JD (2000) Degassing and crystallization of ascending andesite and dacite. In: Francis P, Neuberg J, Sparks RSJ (eds) Causes and consequences of eruptions of andesite volcanoes. Phil Trans R Soc London A, Royal Society, pp 1487-1513
11. Chouet B, Dawson P, Arciniega-Ceballos A (2005) Source mechanism of Vulcanian degassing at Popocate´petl Volcano, Mexico, determined from waveform inversions of very long period signals. J Geophys Res, Vol 110, B07301, doi:10.1029/2004JB003524

12. Christiansen RL, Peterson DW (1981) Chronology of the 1980 Eruptive Activity. In: P.W. Lipman P, Mullineaux DR (eds) The 1980 Eruptions of Mount St. Helens, Washington, U.S. Geological Survey Professional Paper 1250, 844 p

13. Clarke AB, Stephens S, Teasdale R, Sparks RSJ, Diller K (2007) Petrological constraints on the decompression history of magma prior to Vulcanian explosions at the Soufrière Hills volcano, Montserrat. J Volcanol Geotherm Res, Vol 161, pp 261-274, doi: 10.1016/j.jvolgeores.2006.11.007

14. Cole P, Calder ES, Sparks RSJ, Clarke AB, Druitt TH, Young SR, Herd R, Harford CL, Norton GE (2002) Deposits from dome-collapse and fountain-collapse pyroclastic flows at Soufrière Hills Volcano, Montserrat. In: Druitt TH, Kokelaar BP (eds) The eruption of the Soufrière Hills Volcano, Montserrat from 1995 to 1999. Geological Society, London, Memoir No 21, pp. 231 – 262

15. Connor CB, Sparks RSJ, Mason RM, Bonadonna C, Young SR (2003) Exploring links between physical and probabilistic models of volcanic eruptions: the Soufriere Hills Volcano, Montserrat. Geophys Res Lett, Vol 30, doi: 10.1029/2003 GLO17384

16. Costa A (2005) Viscosity of high crystal content melts: dependence on solid fraction, Geophys Res Lett, Vol 32, No L22308, doi: 10.1029/2005GL02430

17. Costa A, Macedonio G (2002) Nonlinear phenomena in fluids with temperature-dependent viscosity: an hysteresis model for magma flow in conduits. Geophys Res Lett, Vol 29, No 10, doi:1029/2001GL014493

18. Costa A, Macedonio G (2003) Viscous heating in fluids with temperature-dependent viscosity: implications for magma flows. Nonlinear Proc Geophys, Vol 10, pp 545–555

19. Costa A, Macedonio G (2005) Viscous heating in fluids with temperature-dependent viscosity: triggering of secondary flows. J Fluid Mech, Vol 540, pp 21–38.

20. Costa A, Melnik O, Sparks RSJ (2007) Controls of conduit geometry and wallrock elasticity on lava dome eruptions. Earth Planet Sci Lett, Vol 260, pp 137-151, doi: 10.1016/j.epsl.2007.05.024

21. Costa A, Melnik O, Sparks RSJ, Voight B (2007) The control of magma flow in dykes on cyclic lava dome extrusion. Geophys Res Lett, Vol 34, No L02303, doi:1029/2006GL027466

22. Couch S, Sparks RSJ, Carroll MR (2001) Mineral disequilibrium in lavas explained by convective self-mixing in open magma chambers, Nature, Vol 411, pp 1037-1039

23. Denlinger RP, Hoblitt RP (1999) Cyclic eruptive behaviour of silicic volcanoes, Geology, Vol 27, No 5, pp 459-462

24. Diller K., A. B. Clarke, B. Voight, A. Neri (2006), Mechanisms of conduit plug formation: Implications for vulcanian explosions, Geophys. Res. Lett., 33, L20302, doi:10.1029/2006GL027391

25. Dirksen O, Humphreys MCS, Pletchov P, Melnik O, Demyanchuk Y, Sparks RSJ, Mahony S (2006) The 2001-2004 dome-forming eruption of Shiveluch Volcano, Kamchatka: Observation, petrological investigation and numerical modelling, J Volcanol Geotherm Res, Vol 155, pp 201-226, doi:10.1016/j.jvolgeores.2006.03.029

26. Druitt TH, Young S, Baptie B, Calder E, Clarke AB, Cole P, Harford C, Herd R, Luckett R, Ryan G, Sparks RSJ, Voight B (2002) Episodes of cyclic Vulcanian explosive activity with fountain collapse at Soufrière Hills volcano, Montserrat. In: Druitt TH, Kokelaar BP (eds) The eruption of the Soufrière Hills Volcano, Montserrat from 1995 to 1999. Geological Society, London, Memoir No 21, pp 231-262

27. Eichelberger JC, Carrigan CR, Westrich HR, Price RH (1986) Non-explosive silicic volcanism. Nature, Vol 323, pp 598-602

28. Fedotov SA, Dvigalo VN, Zharinov NA, Ivanov VV, Seliverstov NI, Khubunaya SA, Demyanchuk YV, Markov LG, Osipenko LG, Smelov NP (2001) The eruption of Shiveluch volcano on May- July 2001. Volcanol and Seismol, Vol 6, pp 3-15

29. Fink JH, Griffiths RW (1990) Radial spreading of viscous gravity currents with solidifying crust. J Fluid Mech, Vol 221, pp 485-509

30. Fink JH, Griffiths RW (1998) Morphology, eruption rates, and rheology of lava domes: Insights from laboratory models. J Geophys Res, Vol 103, pp 527-545

31. Green, D.N.; Neuberg, J. (2006) Waveform classification of volcanic low-frequency earthquake swarms and its implication at Soufrire *H*ills Volcano, Montserrat, Journal of Volcanology and Geothermal Research, 153, pp.51-63. doi:10.1016/j.jvolgeores.2005.08.003

32. Hale AJ, Bourgouin L, Mühlhaus HB (2007) Using the level set method to model endogenous lava dome growth. J Geophys Res, Vol 112, No B03213, doi:10.1029/2006JB004445

33. Hale AJ, Wadge G (2003) Numerical modeling of the growth dynamics of a simple silicic lava dome. Geophys Res Lett, Vol 30, No 19, doi:10.1029/2003GL018182

34. Hammer JE, Rutherford MJ (2002) An experimental study of the kinetics of decompression-induced crystallization in silicic melt. J Geophys Res, Vol 107, No B1, doi:10.1029/2001JB000281

35. Harris AL, Rose WI, Flynn LP (2002) Temporal trends in Lava Dome extrusion at Santiaguito 1922-2000. Bull Volcanol, Vol 65, pp 77-89

36. Hess KU, Dingwell DB (1996) Viscosities of hydrous leucogranite melts: A non-Arrhenian model, Am Mineral, Vol 81, pp 1297-1300

37. Hoblitt RP, Wolfe EW, Scott WE, Couchman MR, Pallister JS, Javier D (1996) The preclimactic eruptions of Mount Pinatubo, June 1991.In: Newhall CG, Punongbayan RS (eds) Fire and Mud: Eruptions and Lahars of Mount Pinatubo, Philippines, Philippine Institute of Volcanology and Seismology, Quezon City, and University of Washington Press, Seattle, pp. 457-511

38. Hort M (1998) Abrupt change in magma liquidus temperature because of volatile loss or magma mixing: effects of Nucleation, crystal growth and thermal history of the magma. J Petrol, Vol 39, pp 1063-1076

39. Humphreys M, Blundy, JD, Sparks RSJ (2006) Magma Evolution and Open-system processes at Shiveluch Volcano: insights from phenocryst zoning. J Petrol, Vol 47, No 12, pp 2303-2334, doi: 10.1093/petrology/eg1045

40. Huppert HE, Shepherd JB, Sigurdsson H, Sparks RSJ (1982) On lava dome growth, with application to the 1979 lava extrusion of the Soufriere, St Vincent. J Volcanol Geotherm Res, Vol 14, pp 199-222

41. Huppert HE, Woods AW (2002) The role of volatiles in magma chamber dynamics. Nature, Vol 420, pp 493-495

42. Ida Y (1996) Cyclic fluid effusion accompanied by pressure change: Implication for volcanic eruptions and tremor. Geophys Res Lett Vol 23, pp 1457-1460

43. Iverson, R. M., et al. (2006), Dynamics of seismogenic volcanic extrusion at Mount St. Helens in 2004–05, Nature, Vol 444, pp 439– 443

44. Jaquet O, Sparks RSJ, Carniel R (2006) Magma Memory recorded by statistics of volcanic explosions at the Soufriere Hills Volcano, Montserrat. In: Mader HM, Coles SG, Connor CB, Connor LJ (eds) Statistics in Volcanology, Geological Society, London, Special Publication of IAVCEI, Vol 1, pp 175-184

45. Jaupart C, Allegre CJ (1991) Gas content, eruption rate and instabilities of eruption regime in silicic volcanoes. Earth Planet Sci Lett,Vol 102, pp 413-429

46. Kirkpatrick R (1976) Towards a Kinetic Model for the Crystallization of Magma Bodies. J Geophys Res, Vol 81, pp 2565–2571

47. Landau L , Lifshitz E (1987) Fluid Mechanics, 2nd ed., Butterworth-Heinmann, Oxford

48. Lejeune A, Richet P (1995) Rheology of crystal-bearing silicate melts: An experimental study at high viscosità. J Geophys Res, Vol 100, pp 4215-4229

49. Lensky NG, Sparks RSJ, Navon O, Lyakhovsky V (2007) Cylic activity at Soufriere Hills volcano. Montserrat. J Volcanol Geotherm Res, (in review)

50. Lister JR, Kerr RC (1991) Fluid mechanical models of crack propagation and their application to magma transport in dykes. J Geophys Res, Vol 96, pp 10049-10077

51. Llewellin EW, Manga M (2005) Bubble suspension rheology and implications for conduit flow. J Volcanol Geotherm Res, Vol 143, pp 205-217

52. Loitsyansky LG (1978) Fluid and gas mechanics. 847 pp, Nauka, Moscow, (in Russian)

53. Maeda I (2000) Nonlinear visco-elastic volcanic model and its application to the recent eruption of Mt. Unzen. J Volcanol Geotherm Res, Vol 95, pp 35-47

54. Mason RM, Starostin AB, Melnik O, Sparks RSJ (2006) From Vulcanian explosions to sustained explosive eruptions: The role of diffusive mass transfer in conduit flow dynamics. J Volcanol Geotherm Res, Vol 153, pp 148-165, doi: 10.1016/j.jvolgeores.2005.08.011

55. Marsh BD (2000) Reservoirs of Magma and Magma chambers, In: Sigurdsson H (ed) Encyclopedia of volcanoes, Academic Press, New York, pp 191–206

56. Mastin GL, Pollard DD (1988) Surface Deformation and Shallow Dike Intrusion Processes at Inyo Craters, Long Valley, California. J Geophys Res, Vol 93, No B11, pp 13221-13235.

57. Matthews SJ, Gardeweg MC, Sparks RSJ (1997) The 1984 to 1996 cyclic activity of Lascar Volcano, northern Chile: Cycles of dome growth, dome subsidence, degassing and explosive eruptions. Bull Volcanol, Vol 59, pp 72– 82

58. Mattioli G, Dixon TH, Farina F, Howell ES, Jansma PE, Smith AL (1998) GPS measurement of surface deformation around Soufriere Hills volcano, Montserrat from October 1995 to July 1996. Geophys Res Lett, Vol 25, No 18, pp 3417-3420

59. Melnik O (2000) Dynamics of two- phase conduit flow of high-viscosity gas-saturated magma: large variations of sustained explosive eruption intensity, Bull Volcanol, Vol 62, pp 153-170

60. Melnik O, Barmin A, Sparks RSJ (2005) Dynamics of magma flow inside volcanic conduits with bubble overpressure buildup and gas loss through permeable magma. J Volcanol Geotherm Res, Vol 143, pp 53–68

61. Melnik O, Sparks RSJ (1999) Non-linear dynamics of lava dome extrusion. Nature, Vol 402, pp 37-41

62. Melnik O, Sparks RSJ (2002) Dynamics of magma ascent and lava extrusion at Soufrière Hills Volcano, Montserrat. In: Druitt TH, Kokelaar BP (eds) The eruption of the Soufrière Hills Volcano, Montserrat from 1995 to 1999. Geological Society, London, Memoir No 21, pp 223-240

63. Melnik O, Sparks RSJ (2005) Controls on conduit magma flow dynamics during lava dome building eruptions, J Geophys Res, 110, B02209, doi:10.1029/2004JB003183

64. Mériaux C, Jaupart C (1995) Simple fluid dynamic models of volcanic rift zones. Earth Planet Sci Lett, Vol 136, pp 223–240

65. Murphy MD, Sparks SJ, Barclay J, Carroll MR, Brewer TS (2000) Remobilization origin for andesite magma by intrusion of mafic magma at the Soufrière Hills Volcano, Montserrat, W.I.: a trigger for renewed eruption. J Petrol, Vol 41, pp 21-42

66. Muskhelishvili N (1963) Some Basic Problems in the Mathematical Theory of Elasticity, Noordhof, Leiden, The Netherlands

67. Nakada S, Eichelberger JC (2004) Looking into a volcano: drilling Unzen. Geotimes, Vol 49, pp 14-17

68. Nakada S, Shimizu H, Ohta K (1999) Overview of the 1990-1995 eruption at Unzen Volcano. J. Volcanol Geoth Res, Vol 89, pp 1-22

69. Navon O, Lyakhovsky V (1998) Vesiculation processes in silicic magmas. In: Gilbert J, Sparks RSJ (Eds) The Physics of explosive volcanic eruption, Geological Society, London, Special Pubblication, Vol 145, pp 27-50

70. Neuberg JW, Tuffen H, Collier L, Green D, Powell T, Dingwell D (2006) The trigger mechanism of low-frequency earthquakes on Montserrat. J Volcanol Geotherm Res, Vol 153, pp 37–50

71. Newhall CG, Melson WG (1983) Explosive activity associated with the growth of volcanic domes. J. Volcanol. Geoth. Res., Vol 17, pp 111-131

72. Norton GE, Watts RB, Voight B, Mattioli GS, Herd RA, Young SR, Devine JD, Aspinall WP, Bonadonna C, Baptie BJ, Edmonds M, Harford CL, Jolly AD, Loughlin SC, Luckett R, Sparks RSJ (2002) Pyroclastic flow and explosive activity of the lava dome of Soufrière Hills volcano, Montserrat, during a period of no magma extrusion (March 1998 to November 1999). In: Druitt TH, Kokelaar BP (eds) The eruption of the Soufrière Hills Volcano, Montserrat from 1995 to 1999. Geological Society, London, Memoir No 21, pp 467-482

73. Ohba T, Kitade Y (2005) Subvolcanic hydrothermal systems: Implications from hydrothermal minerals in hydrovolcanic ash. J Volcanol Geotherm Res, Vol 145, pp 249-262

74. Robertson R, Cole P, Sparks RSJ, Harford C, Lejeune AM, McGuire WJ, Miller AD, Murphy MD, Norton G, Stevens NF, Young SR (1998) The explosive eruption of Soufriere Hills Volcano, Montserrat 17 September, 1996. Geophys Res Lett, Vol 25, pp 3429-3432

75. Roman DC (2005) Numerical models of volcanotectonic earthquake triggering on non-ideally oriented faults, Geophys Res Lett, Vol 32, doi 10.1029/2004GL021549

76. Roman DC, Neuberg J, Luckett RR (2006) Assessing the likelihood of volcanic eruption through analysis of volcanotectonic earthquake fault-plane solutions. Earth Planet Sci Lett, Vol 248, pp 244-252

77. Rubin AM (1995) Propagation of magma-filled cracks. Annu Rev Planet Sci, Vol 23, pp 287-336

78. Saar MO, Manga M, Katharine VC, Fremouw S (2001) Numerical models of the onset of yield strength in crystal–melt suspensions Earth Planet Sci Lett, Vol 187, pp 367-379

79. Sahagian D (2005) Volcanic eruption mechanisms: Insights from intercomparison of models of conduit processes. J Volcanol Geotherm Res, Vol 143, No 1-3, pp 1-15

80. Slezin YB (1984) Dispersion regime dynamics in volcanic eruptions. 2. Flow rate instability conditions and nature of catastrophic explosive eruptions. Vulkanol i Seismol, Vol 1, pp 23-35

81. Slezin YB (2003) The mechanism of volcanic eruptions (a steady state approach). J Volcanol Geotherm Res, Vol 122, pp 7-50

82. Sparks RSJ (1978) The dynamics of bubble formation and growth in magmas – a review and analysis. J Volcanol Geotherm Res, Vol 3, pp 1-37

83. Sparks RSJ (1997) Causes and consequences of pressurization in lava dome eruptions. Earth Planet Sci Lett, Vol 150, pp 177-189

84. Sparks RSJ (2003) Forecasting Volcanic Eruptions. Earth and Planetary Science Letters Frontiers in Earth Science Series, Vol 210, pp 1-15

85. Sparks RSJ, Aspinall WP (2004) Volcanic Activity: Frontiers and Challenges. In: Forecasting, Prediction, and Risk Assessment. AGU Geophysical Monograph "State of the Planet" 150, IUGG Monograph 19, pp 359-374

86. Sparks RSJ, Murphy MD, Lejeune AM, Watts RB, Barclay J, Young SR (2000) Control on the emplacement of the andesite lava dome of the Soufriere Hills Volcano by degassing-induced crystallization. Terra Nova, 12, 14-20

87. Sparks RSJ, Young SR (2002) The eruption of Soufrière Hills volcano, Montserrat (1995-1999): overview of scientific results. In: Druitt TH, Kokelaar BP (eds) The eruption of the Soufrière Hills Volcano, Montserrat from 1995 to 1999. Geological Society, London, Memoir No 21, pp 45-69

88. Sparks RSJ, Young SR, Barclay J, Calder ES, Cole PD, Darroux B, Davies MA, Druitt TH, Harford CL, Herd R, James M, Lejeune AM, Loughlin S, Norton G, Skerrit G, Stevens NF, Toothill J, Wadge G, Watts R (1998) Magma production and growth of the lava dome of the Soufrière Hills Volcano, Montserrat, West Indies: November 1995 to December 1997. Geophys Res Lett, Vol 25, pp 3421-3424

89. Swanson DA, Holcomb RT (1990) Regularities in growth of the Mount St. Helens dacite dome 1980-1986. In: Fink JH (Editor), Lava flows and domes; emplacement mechanisms and hazard implications. Springer Verlag, Berlin, pp 3-24

90. Voight B, Hoblitt RP, Clarke AB, Lockhart AB, Miller AD, Lynch L, McMahon J (1998) Remarkable cyclic ground deformation monitored in real-time on Montserrat, and its use in eruption forecasting. Geophys Res Lett, Vol 25, pp 3405-3408

91. Voight B, Sparks RSJ, Miller AD, Stewart RC, Hoblitt RP, Clarke A, Ewart J, Aspinall W, Baptie B, Druitt TH, Herd R, Jackson P, Lockhart AB, Loughlin SC, Lynch L, McMahon J, Norton GE, Robertson R, Watson IM, Young SR (1999) Magma flow instability and cyclic activity at Soufrière Hills Volcano, Montserrat. Science, Vol 283, pp 1138-1142

92. Walker GPL (1973) Lengths of lava flows. Philos Trans Royal Soc A, Vol 274, pp 107-118

93. Watson IM et al (2000) The relationship between degassing and ground deformation at Soufriere Hills Volcano, Montserrat. J Volcanol Geotherm Res, Vol 98, No 1-4, pp 117-126

94. Watts RB, Sparks RSJ, Herd RA, Young SR (2002) Growth patterns and emplacement of the andesitic lava dome at Soufrière Hills Volcano, Montserrat. In: Druitt TH, Kokelaar BP (eds) The eruption of the Soufrière Hills Volcano, Montserrat from 1995 to 1999. Geological Society, London, Memoir No 21, pp 115-152

95. Whitehead JA, Helfrich KR (1991) Instability of flow with temperature-dependent viscosity : a model of magma dynamics. J Geophys Res, Vol 96, pp 4145-4155

96. Williams SN, Self S (1983) The October 1902 Plinian eruption of Santa Maria volcano, Guatemala. J Volcanol Geotherm Res, Vol 16, pp 33-(Melnik and Sparks, 2005)

97. Woods AW, Koyaguchi T (1994) Transitions between explosive and effusive eruption of silicic magmas, Nature, Vol 370, pp 641-645

98. Wylie JJ, Voight B, Whitehead JA (1999) Instability of magma flow from volatile-dependent viscosity, Science, Vol 285, pp 1883-1885

99. Yokoyama I, Yamashita H, Watanabe H, Okada H, Geophysical characteristics of dacite volcanism - 1977-1978 eruption of Usu volcano. J Volcanol Geotherm Res, Vol 9, pp 335-358

Books and Reviews

Dobran F (2001) Volcanic Processes: Mechanisms In Material Transport, Springer, pp 620

Gilbert, J.S. and Sparks, R.S.J. (eds) (1998) The Physics of Explosive Volcanism. Special Publication of the Geological Society of London, pp186 p

Gonnermann H, Manga M (2007) The fluid mechanics inside a volcano, Annual Reviews of Fluids Mechanics, vol. 39, 321-356

Mader HM, Coles SG, Connor CB, Connor LJ (2006) Statistics in Volcanology. IAVCEI Publications, Geological Society Publishing House, pp 296

Figure captions

Figure 1. Schematic view of the volcanic system. In the upper part the conduit is cylindrical with a radius R. A transition from the cylinder to a dyke occurs at depth L_T. The length scale for the transition from cylinder to dyke is w_T. The dyke has an elliptical cross-section with semi-axis lengths a_0 and b_0. The chamber is located a depth L. In the text we used also the following auxiliary variables: $D = 2R$ for conduit diameter, $L_d = L - L_T$ for the dyke vertical length, $W_d = 2a_0$ for the dyke width, and $H_d = 2b_0$ for the dyke thickness. After [20].

Figure 2. Seismic and tilt data for eruptions of Mount Pinatubo and the Soufriere Hills Volcano Montserrat (after [23] and [90]).

Figure 3. Observed discharge rate versus time for (a) Mount St Helens dome growth and (b) Santiaguito volcano and Shiveluch (c).

Figure 4. The general steady-state solution and possible quasi-static evolution of an eruption. After [3].

Figure 5. Discharge rate versus time for (a) Mount St Helens dome growth and (b) Santiaguito volcano. In dots are the observed values of discharge rates and the solid line are best fit simulations. After [3].

Figure 6. (a) Steady-state solutions and dependence of discharge rate on time for Newtonian and Bingham rheology of the magma. Yield strength is a parameter marked on the curves (values in MPa). For Bingham rheology discharge rate remains zero between the pulses of activity. Bingham rheology results in much higher chamber pressures prior to the onset of activity and, therefore, much higher discharge rates in comparison with Newtonian rheology. (b) Comparison of the period of pulsation in discharge rate for Newtonian and Bingham rheologies. After [63].

Figure 7. (a) Comparison of calculated and measured discharge rates (a) and volumes of the dome (b) for the episode of the dome growth in 2001– 2002. Influx into the magma chamber is shown by a dashed line in (a). Time in days begins on 6th June, 2001. After [25].

Figure 8. (a) Dependence of magma discharge rate (solid line) and magmatic overpressure at depth of 1 km (dashed line) on time, for a= 240 m and b = 2.25 m at the inlet of the dyke. The period of

cycle is 46 days, average discharge rate is 6.2 m^3/s, with peak rate about 12 m^3/s. (b) Profiles of cross-section areas of the conduit during one cycle. Curve A corresponds to the beginning of the cycle, B - to a point on the curve of ascending discharge rate, C - to maximum discharge, and D to the middle of descending discharge curve. At the beginning of the cycle, due to large viscosity of magma (at low discharge rate crystal content is high) large magmatic overpressure develops, reaching a maximum near the transition between the dyke and cylindrical conduit; the dyke inflates providing temporary magma storage. Minimum dyke volume corresponds to maximum discharge rate (curve C). After [21].

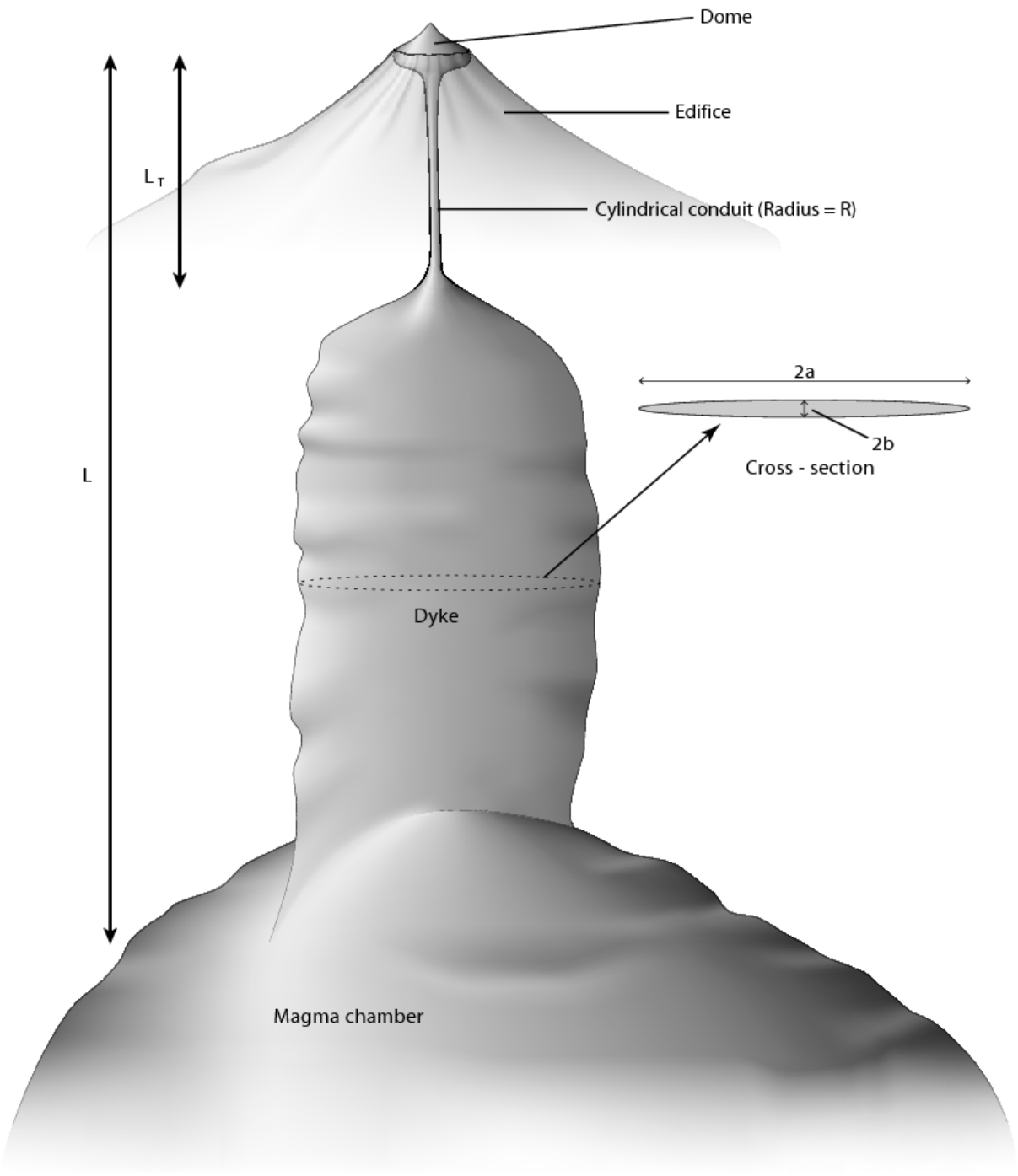
Dome
Edifice
L_T
Cylindrical conduit (Radius = R)
2a
2b
Cross - section
L
Dyke
Magma chamber

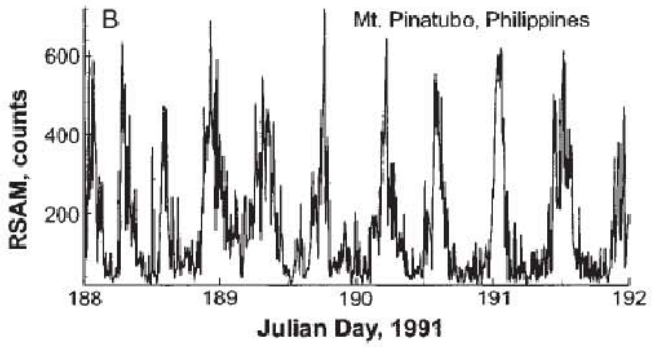
B
Mt. Pinatubo, Philippines
RSAM, counts
600
400
200
188
189
190
191
192
Julian Day, 1991

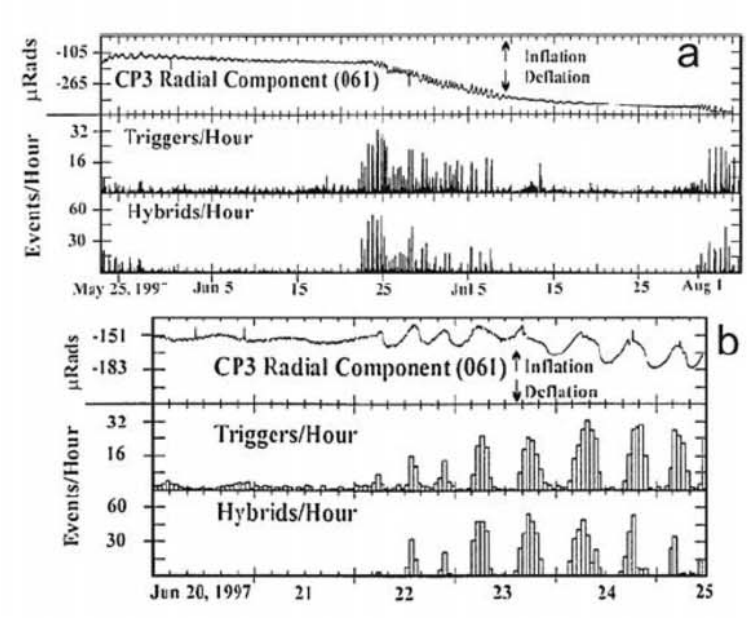
μRads
-105
-265
CP3 Radial Component (061)
Inflation
Deflation
a
Events/Hour
32
16
Triggers/Hour
60
30
Hybrids/Hour
May 25, 199
Jun 5
15
25
Jul 5
15
25
Aug 1
μRads
-151
-183
CP3 Radial Component (061)
Inflation
Deflation
b
Events/Hour
32
16
Triggers/Hour
60
30
Hybrids/Hour
Jun 20, 1997
21
22
23
24
25

Mount St Helens (USA)

Santiaguito (Guatemala)

Shiveluch (Russia)

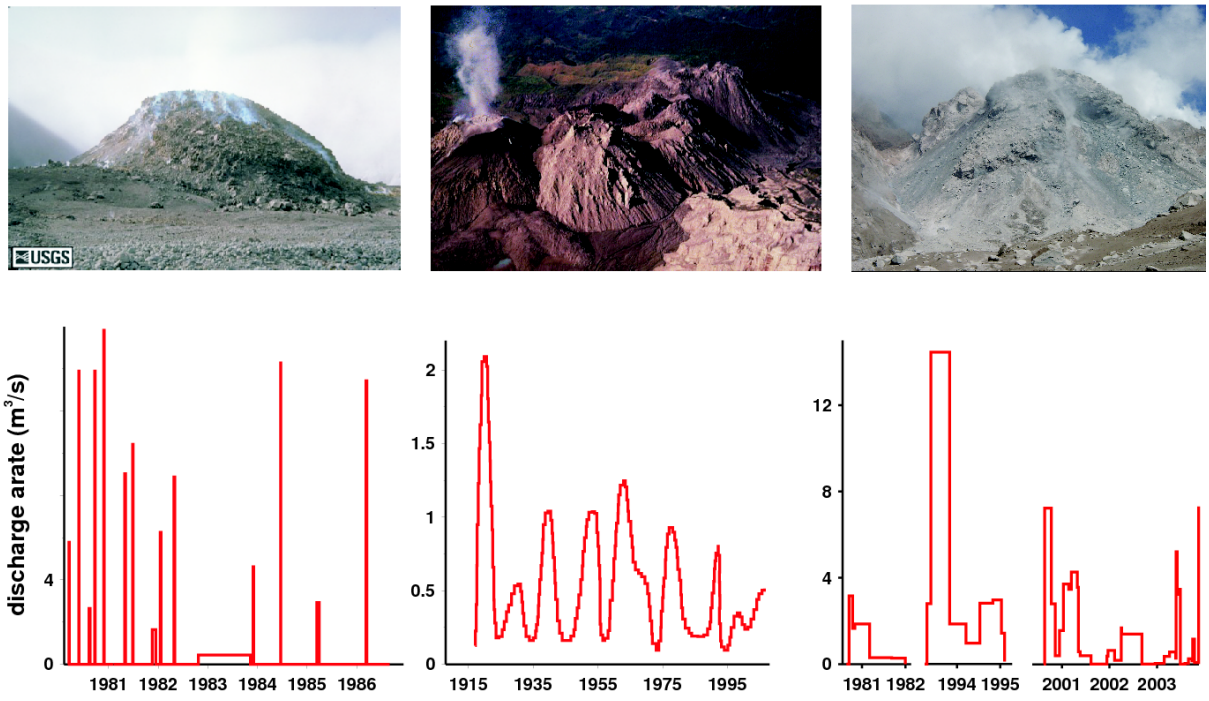

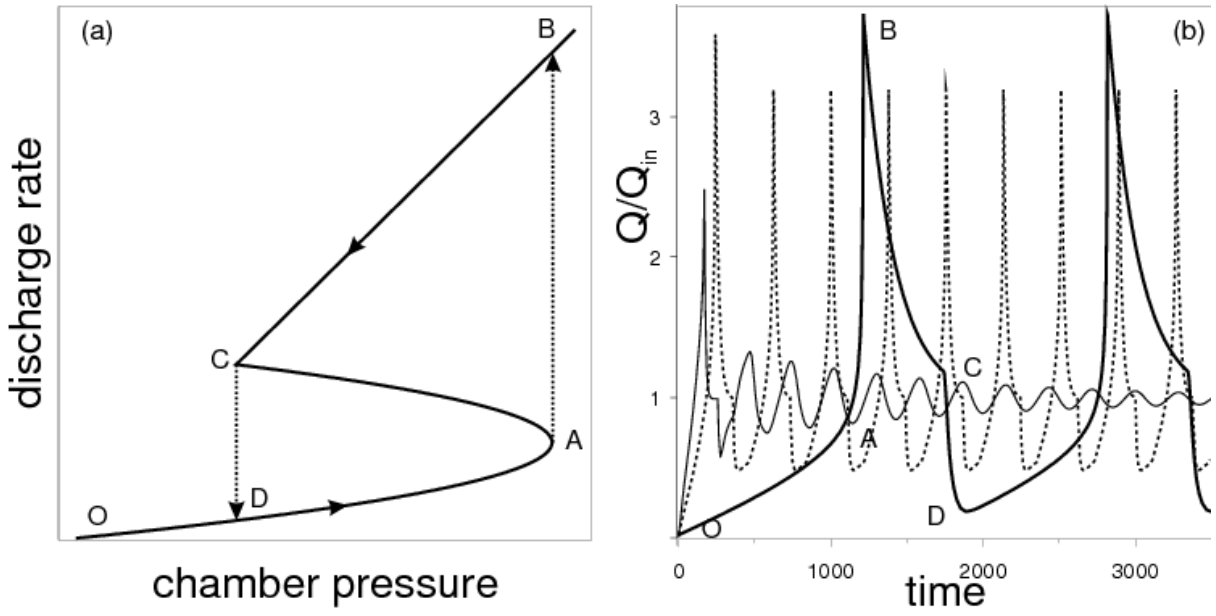
(a)
B
C
A
D
O
discharge rate
chamber pressure
(b)
B
C
A
D
O
Q/Q_{in}
3
2
1
0
1000
2000
3000
time

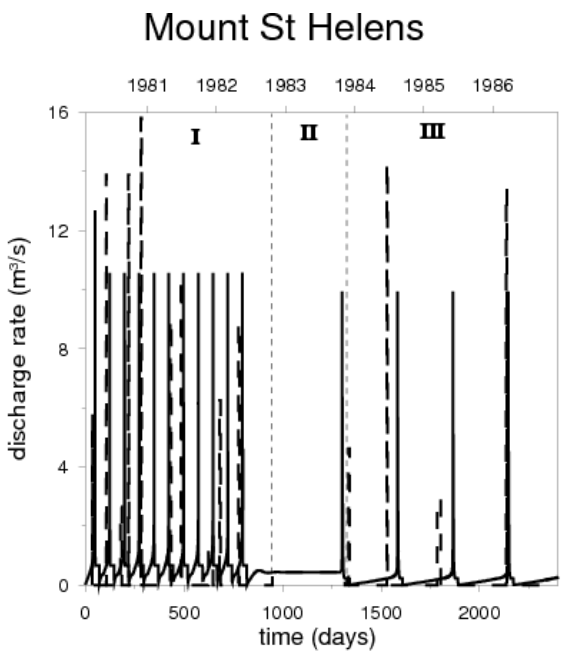
Mount St Helens
1981
1982
1983
1984
1985
1986
I
II
III
discharge rate (m³/s)
time (days)
0
4
8
12
16
500
1000
1500
2000

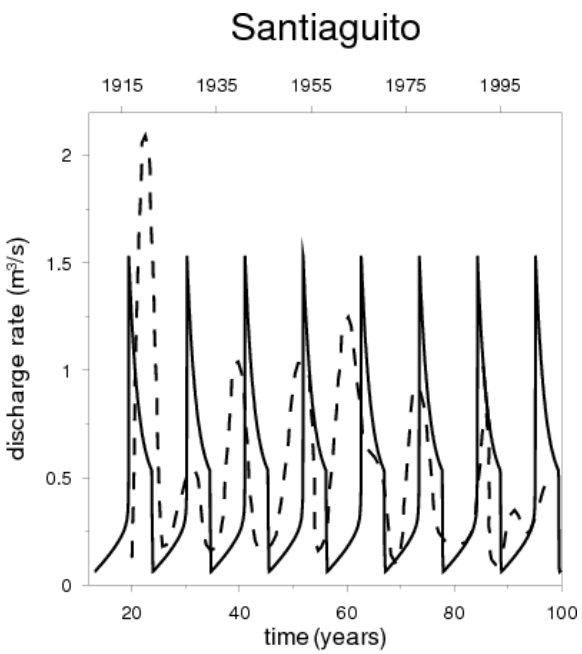
Santiaguito
1915
1935
1955
1975
1995
discharge rate (m³/s)
time (years)
0
0.5
1
1.5
2
20
40
60
80
100

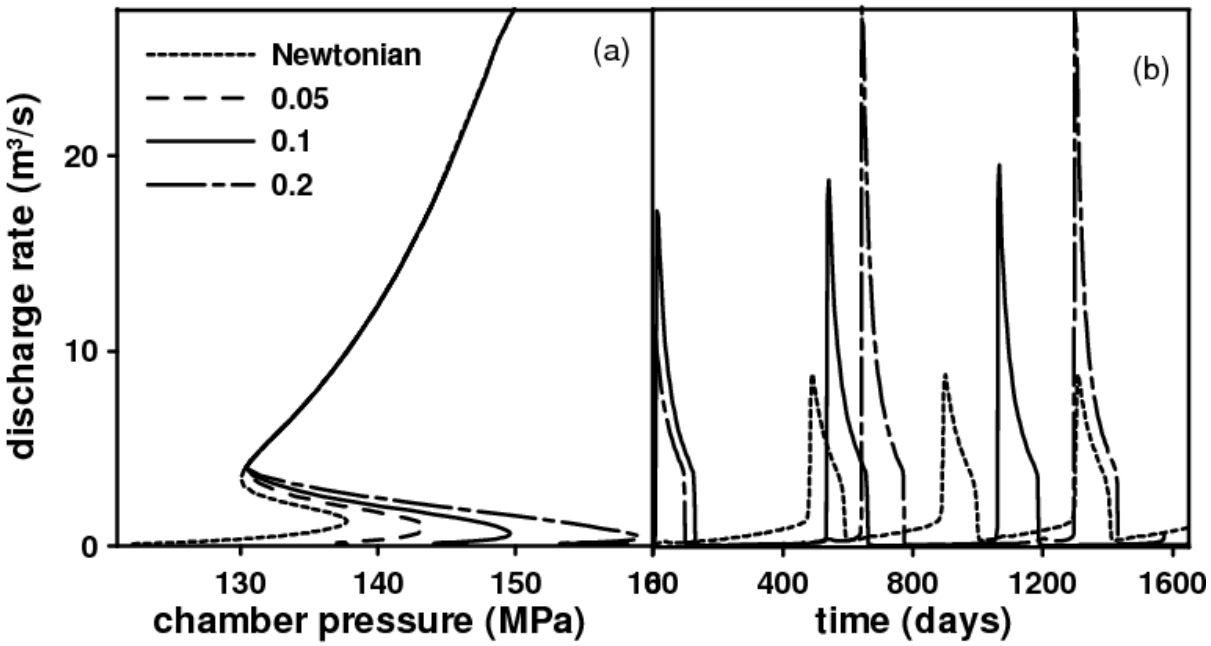
Newtonian
0.05
0.1
0.2
(a)
(b)
discharge rate (m³/s)
0
10
20
130
140
150
160
chamber pressure (MPa)
400
800
1200
1600
time (days)

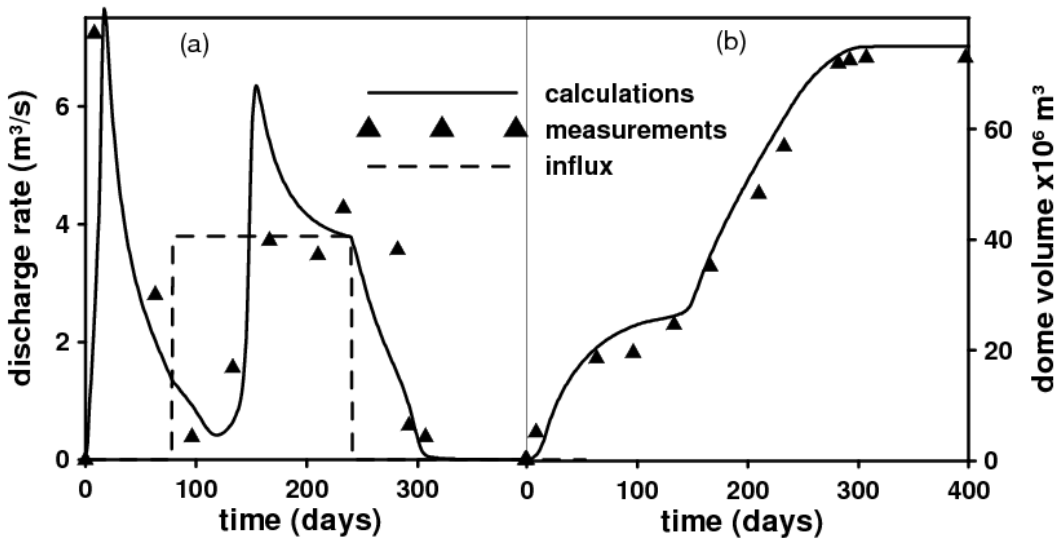
(a)
(b)
calculations
measurements
influx
discharge rate (m³/s)
dome volume x10⁶ m³
time (days)
time (days)
0
2
4
6
0
20
40
60
0
100
200
300
0
100
200
300
400

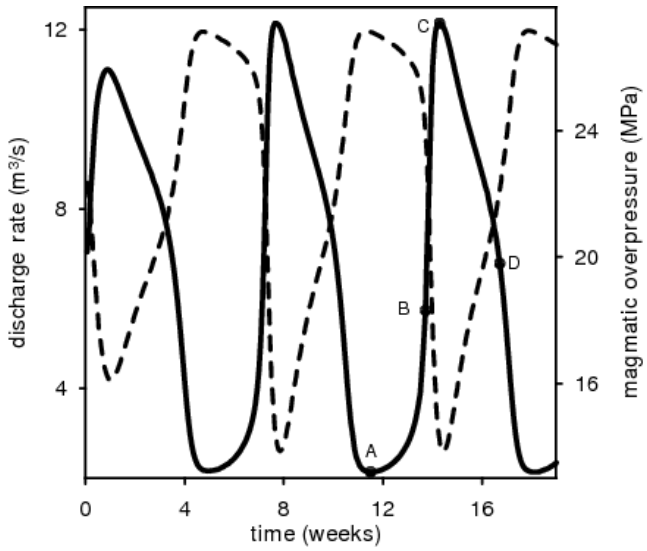
discharge rate (m³/s)
magmatic overpressure (MPa)
time (weeks)
A
B
C
D

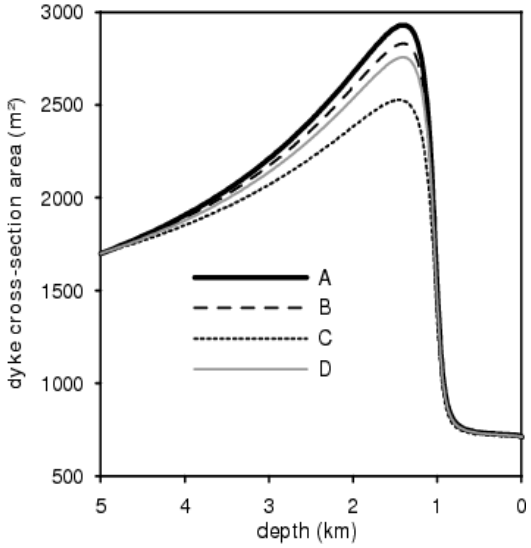
dyke cross-section area (m²)
depth (km)
A
B
C
D